AD_____

Award Number: W81XWH-04-1-0168

TITLE: PSES-a Novel Prostate Specific Chimeric Enhancer for Prostate Cancer Gene Therapy

PRINCIPAL INVESTIGATOR: Chinghai Kao, Ph.D.

CONTRACTING ORGANIZATION: Indiana University
Indianapolis, IN 46202-5167

REPORT DATE: February 2007

TYPE OF REPORT: Final

PREPARED FOR: U.S. Army Medical Research and Materiel Command
Fort Detrick, Maryland 21702-5012

DISTRIBUTION STATEMENT: Approved for Public Release;
Distribution Unlimited

REPORT DOCUMENTATION PAGE

Form Approved
OMB No. 0704-0188

1. REPORT DATE	2. REPORT TYPE	3. DATES COVERED
01-02-2007	Final	12 Jan 2004 – 11 Jan 2007

4. TITLE AND SUBTITLE

PSES-a Novel Prostate Specific Chimeric Enhancer for Prostate Cancer Gene Therapy

5a. CONTRACT NUMBER

5b. GRANT NUMBER
W81XWH-04-1-0168

5c. PROGRAM ELEMENT NUMBER

6. AUTHOR(S)

Chinghai Kao, Ph.D.

Email: chkao@iupui.edu

5d. PROJECT NUMBER

5e. TASK NUMBER

5f. WORK UNIT NUMBER

7. PERFORMING ORGANIZATION NAME(S) AND ADDRESS(ES)

Indiana University
Indianapolis, IN 46202-5167

8. PERFORMING ORGANIZATION REPORT NUMBER

9. SPONSORING / MONITORING AGENCY NAME(S) AND ADDRESS(ES)
U.S. Army Medical Research and Materiel Command
Fort Detrick, Maryland 21702-5012

10. SPONSOR/MONITOR'S ACRONYM(S)

11. SPONSOR/MONITOR'S REPORT NUMBER(S)

12. DISTRIBUTION / AVAILABILITY STATEMENT
Approved for Public Release; Distribution Unlimited

13. SUPPLEMENTARY NOTES
Original contains colored plates: ALL DTIC reproductions will be in black and white.

14. ABSTRACT

Recently we generated a chemic prostate specific promoter, called PSES, by combining the enhancer elements from the PSA and PSMA genes. Based on PSES, we developed a prostate-restricted replicative adenovirus (PRRA), called AdE4PSESE1a. AdE4PSESE1a only replicated in PSA/PSMA positive prostate cancer cells or cells expressing adenoviral E1 and E4 proteins. AdE4PSESE1a only partially inhibited tumor growth when tested in animals. Then we armed AdE4PSESE1a with TRAIL to make AD-IU-2. Ad-IU-2 retains the prostate specificity of AdE4PSESE1a and expresses TRAIL only in PSA/PSMA positive cells. Ad-IU-2 demonstrated better in vitro cell killing activity and tumor killing activity in vivo than AdE4PSESE1a against PSA/PSMA positive prostate cancers. We also tested whether antiangiogenic factor EndoAngio (an endostatin-angiostatin fusion protein) can slow down tumor growth to give AdE4PSESE1a enough time to eradicate a tumor. We found that co-injection of an EndoAngioexpressing replication defective adenovirus, AdEndoAngio, with AdE4PSESE1a would be able to eliminate 7 of 8 treated tumors. We incorporated EndoAngio expression cassette into AdE4PSESE1a to make an antiangiogenic PRRA.

15. SUBJECT TERMS
TRANSCRIPTIONAL REGULATION OF ADENOVIRAL REPLICATION, GENE THERAPY, PSES CHIMERIC PROMOTER, TISSUE RESTRICTED REPLICATION COMPETENT ADENOVIRUS, TRAIL

16. SECURITY CLASSIFICATION OF:			17. LIMITATION OF ABSTRACT	18. NUMBER OF PAGES	19a. NAME OF RESPONSIBLE PERSON
a. REPORT	b. ABSTRACT	c. THIS PAGE			USAMRMC
U	U	U	UU	51	19b. TELEPHONE NUMBER *(include area code)*

TABLE OF CONTENTS

INTRODUCTION

Metastatic human prostate cancer (PC) is commonly treated by hormone, radiation, and/or chemotherapy. Inevitably, these patients will eventually relapse and develop androgen-independent disease with osseous metastasis. Since no effective therapy is presently available for the treatment of PC metastasis, we are developing a novel gene therapy modality for hormonal refractory prostate cancer based on several prostate specific enhancer cores, AREc3, PSME(del2) and PSES, generated in my laboratory. In this study, we propose to generate an apoptosis inducer, TRAIL (tumor necrosis factor-related apoptosis-inducing ligand), armed prostate restricted replicative adenovirus (PRRA) to treat androgen-independent prostate cancers. Specific Aim 1 will continue our examination into whether PSES chimeric enhancer retains prostate specific activity useful for driving the expression of therapeutic gene to treat AI prostate cancers. Specific Aim 2 will construct several PRRAs based on AREc3/PSMEdel2 or PSES enhancers and investigate their tissue specificity and tumor-killing activity. Specific Aim 3 will arm PRRA with an apoptosis inducer, Trail, to enhance the tumor killing activity of PRRA.

BODY

Task 1. To test the tissue specificity of the PSES chimeric enhancer. (Months 1-12):

a. Test the tissue-specificity of Ad-PSES-Luc in tissue culture cells (Months 1-8). We did not continue this investigation due to difficulty in culturing normal human cells from different organs. We spent quite a lot of money without luck culturing normal cells.

b. Test the tissue specificity of Ad-PSES-Luc in animals (Months 9-12).

Androgen-independent CWR22rv prostate tumors were established in nude mice and treated with 5.7 x 10^9 virus particles of Ad-CMV-luciferase (■) or Ad-PSES-luciferase (□) via tail vein injection. After 2 days, tumors and organs were harvested from sacrificed mice and homogenized. Protein extract was used for luciferase assay. Three mice were used for each group. Ad-CMV-Luc demonstrated high activity in tumors and low activity in liver, lung and spleen. Kidney and prostate showed the lowest activity in all organs tested. This result is consistent with the

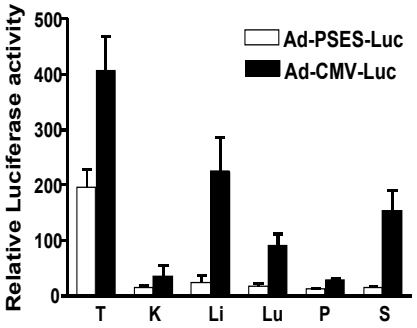

Figure 1. D. 5.7 x 10^9 virus particles of Ad-CMV-luciferase (■) or Ad-PSES-luciferase (□) were injected into the tail vein of mice. After 2 days, tumors and organs were harvested from sacrificed mice and homogenized. Protein extract was used for luciferase assay. Three mice were used for each group. Results are presented as mean ± S.D. Luciferase activity was presented as per mg protein. T: tumor; K: kidney; Li: liver; Lu: lung; P: prostate; S: spleen.

reported virus distribution study and our prior results. As expected, Ad-PSES-Luc also has high activity in tumor, and its activity in liver, lung and spleen is much lower than Ad-CMV-Luc. The activity of Ad-PSES-Luc in prostate and kidney is similar to the background signal.

Task 2. To investigate the capability of PSA and PSMA enhancer to drive adenovirus replication in a prostate cancer-specific manner (Months 1-24):

a. Construct and amplify AREc3/PSME(del2) restricted replicative adenoviruses (Months 1-8).

We generated an AREc3/PSME(del2) restricted replicative adenovirus, AdE4PSESE1a, by putting the PSES and E1a gene in the E4 region **(see Figure 1 in attached paper 1).** A CMV-EGFP expression cassette was inserted in front of the E1b gene.

b. In vitro test of tissue-specific expression of E1a and E1b by AREc3/PSME(del2) restricted replicative adenoviruses (Months 9-12).

AdE4PSESE1a derived E1a and E4 expression in PSA/PSMA positive cells **(see Figure 4 in attached paper 1).**

c. In vitro test of tissue-specific replication of AREc3/PSME(del2) restricted replicative adenoviruses (Months 11-14).

We then tested the tissue specific activity of AdE4PSESE1a on several PSA/PSMA-positive and negative cells. Cells were infected with AdE4PSESE1a and monitored daily under a fluorescent microscope up to 5 days. EGFP expression represented AdE4PSESE1a infection. At 1 day after infection, EGFP-expressing cells were easily detected in all cell types tested **(see Figure 5 in attached paper 1).** The number and intensity of green cells increased in PSA/PSMA-positive prostate cancer cells, but not in PSA/PSMA-negative cells. At day 5, a comet-like patch of green cells had formed only in PSA/PSMA-positive prostate cancer cells. At the same time, we could detect virus plaques under a light microscope. This result and a viral replication assay **(see Table 1 in attached paper 1)** clearly demonstrate that AdE4PSESE1a only replicates efficiently in cells either providing endogenous E4 gene products,

such as 911E4 cells, or allowing E4 expression from the Ad genome, such as C4-2 cells. This established a proof of principle that the E4 gene can be used to control Ad replication.

d. In vitro test of the therapeutic efficacy of AREc3/PSME(del2) restricted replicative adenoviruses (Months 13-16).

To test the tissue/tumor-specific killing activity of AdE4PSESE1a, serial dilutions of AdE4PSESE1a and Ad-wt were applied to C4-2, CWR22rv, PC-3, DU145, HeLa, LoVo, A549, MCF10A and HEK293 in 96-well plates. Cells were monitored under the microscope daily. AdE4PSESE1a was able to kill PSA/PSMA positive C4-2 and CWR22rv at the same doses as Ad-wt. On the other hand, AdE4PSESE1a required 100-fold more virus than Ad-wt to kill LoVo, 500-fold more to kill DU145 and HeLa, 1,000-fold more virus to kill PC-3 and MCF10A, and 10,0000-fold more viruses to kill HEK293 cells. This result indicates that the killing activity for AdE4PSESE1a was the same as Ad-wt for PSA/PSMA-positive cancer cells, and significantly attenuated for PSA/PSMA-negative prostate cancer cells and non-prostatic cancer cells **(see Figure 6 in attached paper 1).**

e. In vivo test of the therapeutic efficacy of AREc3/PSME(del2) restricted replicative adenovirus (Months 17-22).

CWR22rv subcutaneous tumors were established in athymic nude mice**.** The mice were castrated three days after CWR22rv inoculation to test whether AdE4PSESE1a was able to eliminate AI tumors in a castrated host. Mice were randomized 3 weeks after cell inoculation (9 tumors from 6 mice in each group) and received intra-tumoral injections of $2x10^7$ ifu (determined by Adeno-XTM Rapid Titer System from Invitrogen) of AdE4PSESE1a or AdCMV-EGFP (a replication-deficient adenovirus used as a negative control). In addition, 7 tumors from 6 mice were treated intravenously with $5x10^7$ ifu of AdE4PSESE1a twice at a one-week interval. Tumor sizes were monitored once a week. The result demonstrates that tumor growth was significantly retarded in the AdE4PSESE1a-treated groups regardless of the route of viral injection, compared to the AdCMV-EGFP-treated group (**see Figure 7 in attached paper**

1). We frequently observed complete responses to AdE4PSESE1a therapy. For example, 2 tumors disappeared in the AdE4PSESE1a intra-tumoral injection group (**see Figure 7 in attached paper 1**), and 3 tumors disappeared in the tail vein injection group (see Figure 7 in attached paper) in this study. However, the growth inhibitory effects were temporary and the majority of tumors eventually grew back even in animals treated via tail vein injection (**see Figure 7, 8 and 9 in attached paper 1**).

Task 3. To Arm AREc3/PSME(del2) restricted replicative adenovirus with Trail (Months 13-34):

a. Construct and amplify Trail-armed AREc3/PSME(del2) restricted replicative adenovirus (Months 13-18).

We placed TRAIL cDNA at the left ITR under control of the bidirectional PSES enhancer to make a TRAIL armed prostate-restricted-replicative adenovirus, Ad-IU-2. To avoid interference with the adenoviral packaging signal (ψ), *E1a* was placed at the right ITR under the transcriptional control of PSES along with *E4* (**see Figure 1 in attached paper 2**).

b. In vitro test of the therapeutic efficacy of Trail-armed AREc3/PSME(del2) restricted replicative adenovirus. (Months 19-22).

Ad-IU-2 was able to induced apoptosis and kill PSA/PSMA positive cells, but spares normal fibroblasts (**see Figure 2 and 3 in attached paper 2**).

c. In vivo test of the therapeutic efficacy of Trail-armed AREc3/PSME(del2) restricted replicative adenovirus. (~222 animals will be used) (Months 23-28).

Ad-IU-2 demonstrated superior tumor killing activity to plain prostate-restricted replicative adenovirus on CWR22rv s.c. tumors (**see Figure 4 in attached paper 2**).

d. Establish a chimeric tumor model with both PSA/PSMA positive and negative prostate cancer cells. (~100 animals will be used) (Months 25-28).

We generated four fluorescent protein tagged prostate cancer cell lines, PSA/PSMA positive C4-2Red and CWR22rvRed and PSA/PSMA negative PC-3Red and DU145Red. When PSA/PSMA positive and negative cells were co-injected into nude mice, PSA/PSMA negative cells always took over and became the dominant cell type in the hybrid tumor. We failed to establish a chimeric tumor model with both PSA/PSMA positive and negative prostate cancer cells.

e. In vivo test of the bystander killing effect of Trail-armed AREc3/PSME(del2) restricted replicative adenovirus. (~66 animals will be used) (Months 29-34).

Although we could not establish a hybrid tumor model to test the bystander killing effect of Ad-IU-2 (see above), we conducted in vitro experiments to demonstrate the bystander killing effect of Ad-IU-2 (Figure 1).

Figure 1

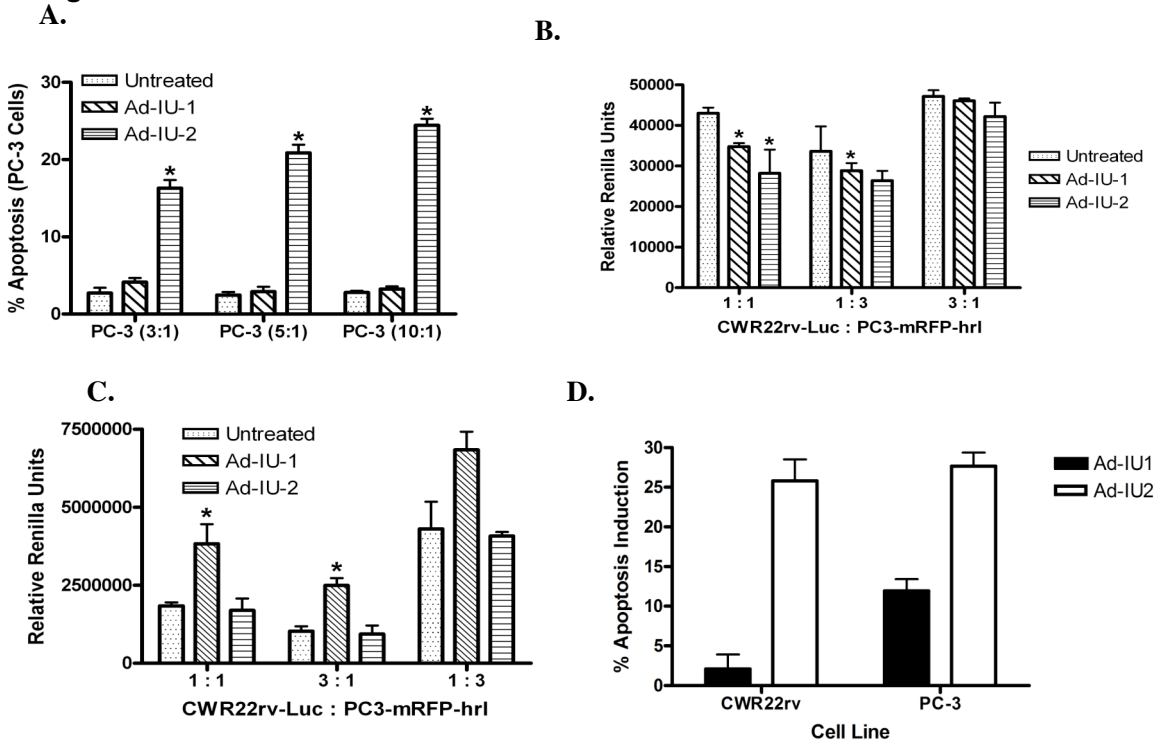

Figure 1. *In vitro* demonstration of a TRAIL-mediated bystander effect. A, PSA/PSMA positive CWR22rv cells were plated in a 12-well plate and infected with 100 vp Ad-IU-1 or Ad-IU-2 24 hours later. Twenty-four hours after infection, the wells were washed 3X with 1X PBS. Following the washing, mRFP-hrl stably transfected PSA/PSMA-negative PC-3 cells were co-plated in the indicated ratios. The percentage of apoptotic PC-3 cells was measured by FACS analysis. Ad-IU-2 significantly induced apoptosis in PC-3 cells compared to basal levels and Ad-IU-1 treated cells, $p = <0.05$. Previously, we demonstrated that direct infection of PC-3 with Ad-IU2 does not result in apoptosis induction. This is expected, as TRAIL expression is minimal in this PCa cell line. Human firefly luciferase stably transfected CWR22rv were plated in a 12-well plate and infected with 100 vp Ad-IU-1 or Ad-IU-2 24 hours later. Twenty-four hours after infection, the wells were washed 3X with 1X PBS. Following the washing, mRFP-hrl stably transfected PC-3 cells were co-plated in the indicated ratios. B, Cells were lysed and luciferase assay was performed after 7 days in co-culture. A decrease in luciferase activity represented a decrease in CWR22rv cell count as compared to the untreated group. C, A decrease in renilla activity represented a decrease in PC-3 cell count, $n = 4$ each group, * = $p<0.05$. Both Ad-IU1 and Ad-IU2 result in direct killing of CWR22rv cells, allowing PC-3 to repopulate the plate; only Ad-IU2-infected co-culture was successful in preventing this PC-3 overgrowth. D, to strengthen this argument, CWR22rv cells were infected with 1000 MOI Ad-IU1 or Ad-IU2 for 48 hrs, after which the conditioned media was harvested and heat-inactivated for virus inactivation at 56^{o}C for 30 min. CWR22rv or PC-3 cells were treated with conditioned media for 24 hrs, then analyzed for apoptosis by AnnexinV/PI FACS analysis. 5-fold induction above that of Ad-IU1 conditioned media was achieved in CWR22rv and 2-fold induction in PC-3 cells.

Task 4. To organize data for report: (Months 35-36)

Most of the data have been published, and the remaining data will be submitted for publication.

Other reportable outcomes.

We also tested whether anti-angiogenic therapy can enhance the tumor killing activity of PSES-based PRRA (Cancer Res 65:1941, 2005). We co-injected a replication defective adenovirus, AdEndoAngio, expressing an anti-angiogenic protein, EndoAngio (endostatin-angiostatin fusion protein) with the PSES-based PRRA, AdE4PSESE1a. We found that co-injection of AdEndoAngio and AdE4PSESE1a was able to eliminate 7 of 8 treated tumors **(see attached paper 3).**

f. KEY RESEARCH ACCOMPLISHMENTS

1. We demonstrated that Ad-IU-2 infected PSA/PSMA positive cells were able to kill PSA/PSMA negative cells via a bystander killing effect. We are currently preparing a manuscript to publish our study on Trail-armed PRRA, Ad-IU-2.

2. We found that antiangiogenic therapy worked synergistically with prostate restricted replicative adenovirus, AdE4PSESE1a, in eliminating androgen independent prostate tumors. This observation initiated a new research direction to investigate an anti-angiogenic PRRA. This study was published.

REPORTABLE OUTCOMES

Some of the results of this study have been published.

Li, X., et al., Combination therapy of androgen-independent prostate cancer using a prostate restricted replicative adenovirus and a replication-defective adenovirus encoding human endostatin-angiostatin fusion gene. Mol Cancer Ther, 2006. 5(3): p. 676-84.

CONCLUSIONS

In this past year we have re-directed our research effort, looking for therapeutic agents that could enhance the therapeutic efficacy of AdE4PSESE1a or Ad-IU-2. We found that anti-angiogenic therapy worked synergistically with AdE4PSESE1a to eliminate prostate tumors. This observation re-directed our research effort to investigate other antiangiogenic factors for their ability to synergize AdE4PSESE1a's tumor killing activity, and to make antiangiogenic PRRAs.

REFERENCES

Gene Therapy for Prostate Cancer by Controlling Adenovirus *E1a* and *E4* Gene Expression with PSES Enhancer

Xiong Li,[1,5] Yan-Ping Zhang,[1,5] Hong-Sup Kim,[1,5] Kyung-Hee Bae,[1,5] Keith M. Stantz,[3] Sang-Jin Lee,[1,5] Chaeyong Jung,[1,5] Juan A. Jiménez,[1,2,5] Thomas A. Gardner,[1,2,5] Meei-Huey Jeng,[2,4,5] and Chinghai Kao[1,2,5]

Departments of [1]Urology, [2]Microbiology and Immunology, [3]Radiology, [4]Medicine, and [5]Walther Oncology Center, Indiana University School of Medicine, Indianapolis, Indiana

Abstract

PSES is a chimeric enhancer containing enhancer elements from prostate-specific antigen (PSA) and prostate-specific membrane antigen (PSMA) genes that are prevalently expressed in androgen-independent prostate cancers. PSES shows strong activity equivalent to cytomegalovirus (CMV) promoter, specifically in PSA/PSMA-positive prostate cancer cells, the major cell types in prostate cancer in the absence of androgen. We developed a recombinant adenovirus (AdE4P-SESE1a) by placing adenoviral *E1a* and *E4* genes under the control of the bidirectional enhancer PSES and enhanced green fluorescent protein gene for the purpose of intratumoral virus tracking under the control of CMV promoter. Because of PSES being very weak in nonprostatic cells, including HEK293 and HER911 that are frequently used to produce recombinant adenovirus, AdE4PSESE1a can only be produced in the HER911E4 cell line which expresses both *E1* and *E4* genes. AdE4PSESE1a showed similar viral replication and tumor cell killing activities to wild-type adenovirus in PSA/PSMA-positive prostate cancer cells. The viral replication and tumor cell killing activities were dramatically attenuated in PSA/PSMA-negative cells. To test whether AdE4PSESE1a could be used to target prostate tumors *in vivo*, CWR22rv s.c. tumors were induced in nude mice and treated with AdE4PSESE1a via intratumoral and tail vein injection. Compared to tumors treated with control virus, the growth of CWR22rv tumors was dramatically inhibited by AdE4PSESE1a via tail vein injection or intratumoral injection. These data show that adenoviral replication can be tightly controlled in a novel fashion by controlling adenoviral *E1a* and *E4* genes simultaneously with a single enhancer. (Cancer Res 2005; 65(5): 1941-51)

Introduction

Prostate cancer is the most frequently diagnosed cancer in men in the United States, with an estimated incidence of more than 916 new cases and 115 deaths per day. Frequently, patients present with locally advanced disease and/or detectable distant bone metastases at initial diagnosis. The best available treatment for patients with advanced disease is androgen ablation therapy, based on the observations of Huggins and Hodges (1) that clinical prostate cancer is under the trophic influence of male hormones. Tumor regression and improvement of clinical symptoms are temporary and inevitably the disease progresses to an androgen-independent state. Currently, no curative therapy is available for androgen-independent prostate cancers.

Gene therapy provides an attractive opportunity to target androgen-independent prostate cancer. Unlike traditional chemotherapy, it can be designed and customized to target cancers specifically according to our understanding of the disease at a molecular level. We have shown that prostate-specific antigen (PSA) or osteocalcin promoter and human herpes simplex thymidine kinase gene-based therapy inhibits the growth of androgen-independent PSA-producing cells (2–4); however, a number of restrictions limit the efficacy of this type of gene therapy. For example, this therapy only works in proliferating tumor cells and is ineffective for slow-growing cancers like prostate cancer. We further explored prostate-restricted replicative adenoviruses as an aggressive approach to eliminate prostate metastases (5). Compared to the replication-deficient adenovirus, this approach allows the virus to propagate and infect more cells in the tumor mass, which will improve the inadequate *in vivo* infectivity and biodistribution of adenovirus.

The most commonly used strategy to construct a tissue/tumor-restricted replicative adenovirus (TRRA) is to place the adenoviral *E1a* gene under the control of tissue/tumor-specific promoters (5–7). E1a protein is central to the regulation of adenoviral gene expression and viral replication by inactivating the function of tumor suppressor pRB and transactivating late gene promoters. Theoretically, without E1a protein the expression of late gene products would be diminished, preventing propagation of the virus in the cell. Tissue/tumor-specific replication could be achieved by placing *E1a* gene under the control of tissue/tumor-specific promoter; however, leaky replication is frequently observed with this strategy. Controlling both *E1a* and *E1b* genes with a tissue/tumor-specific promoter further improves the tissue/tumor-specific replication of TRRAs (8, 9). Recent studies showed tight regulation of adenoviral replication by placing *E1a* and *E4* genes under the control of two promoters that are either duplicates or distinct (10, 11). Because of the difficulty in finding two active and tightly regulated promoters for a tumor type, and the use of two copies of the same promoter might induce recombination, we developed a new strategy which places both *E1a* and *E4* genes under the control of one single prostate-specific enhancer, PSES.

PSES contains enhancer elements from PSA and prostate-specific membrane antigen (PSMA) genes, the two best studied antigens expressed by the majority of androgen-independent prostate cancers. Delineating the regulatory mechanism of PSA and PSMA expression in androgen-independent prostate cancers, we found that the main prostate-specific enhancer activity of the

Requests for reprints: Chinghai Kao, Department of Urology, Indiana University School of Medicine, Room OPW320, 1001 W. 10th Street, Indianapolis, IN 46202. Phone: 317-278-6873; Fax: 317-278-3432; E-mail: chkao@iupui.edu.

PSA enhancer core lies within a 189-bp region called AREc3 which is located 4.2 kb upstream of the start codon (12). The main prostate-specific enhancer activity of the PSMA enhancer core lies within a 331-bp region located in the third intron of the PSMA encoding gene, called PSME(del2) (12). PSES, a combination of AREc3 and PSME(del2), showed much stronger transcriptional activity than either AREc3 or PSME(del2) alone in the presence or absence of androgen and retained tight prostate-specific activity *in vitro* and *in vivo* with an activity comparable to cytomegalovirus (CMV) promoter in PSA/PSMA-positive cells and a basal activity in all PSA/PSMA-negative cells from a variety of organ tissues (12). We believe that PSES is a better transcriptional regulator than AREc3 and PSME(del2) for developing a prostate-specific replication-competent adenovirus for patients with androgen-independent cancers.

Materials and Methods

Cells and Cell Culture. HEK293 is a transformed human embryonic kidney cell line established by Graham (13) that expresses complementing adenoviral E1 protein supporting the replication of E1-deleted recombinant adenoviruses. HEK293 was maintained in MEM (Invitrogen, Carlsbad, CA) containing 10% fetal bovine serum, 1% penicillin/streptomycin, and 1% MEM nonessential amino acids. HER911 is a human embryonic retinoblast cell immortalized with a plasmid containing adenoviral *E1* gene (bp 79-5,789 of the Ad5 genome). HER911 was cultured in DMEM, supplemented with 10% fetal bovine serum and 1% penicillin/streptomycin (14). HER911E4 is an HER911 derivative that expresses adenoviral E4 protein under the control of *tetR* (15). HER911E4 was maintained in the same medium as HER911 supplemented with 0.1 mg/mL hygromycin B (Calbiochem, San Diego, CA) and 2 μg/mL doxycycline (Sigma, St. Louis, MO). C4-2 is an androgen-independent human prostate cancer cell line derived from LNCaP that retains the expression of androgen receptor, PSA, and PSMA (16). CWR22rv is an androgen-independent prostate cancer cell line derived from an androgen-dependent human xenograft tumor, CWR22s (17). PC-3 is an androgen-independent, androgen receptor-, and PSA-negative human prostate cancer cell line derived from the bone marrow aspirates of a patient with confirmed metastatic disease (18). DU145 is an androgen-independent, androgen receptor-, and PSA-negative human prostate cancer cell line established by Stone et al. (19) from a patient with prostate cancer brain metastases. C4-2, CWR22rv, PC-3, and DU145 were all maintained in RPMI 1640 supplemented with 10% fetal bovine serum and 1% penicillin/streptomycin. MCF10A, a nontumorigenic human mammary epithelial cell line, was cultured in a 1:1 mixture of DMEM and F12 medium (DMEM-F12) in which 500 mL of medium were supplemented with 26.3 mL horse serum (Invitrogen), 500 units penicillin/streptomycin, 0.5 mol/L L-glutamine, 5.36 mg insulin, 10.75 μg EGF, 52.5 μg cholera toxin, and 250 μg hydrocortisone (20). HeLa, a human cervical carcinoma, was maintained in DMEM supplemented with 10% fetal bovine serum and 1% penicillin/streptomycin (21). LoVo, a colon cancer cell (22), was maintained in DMEM supplemented with 10% fetal bovine serum and 1% penicillin/streptomycin. All cells were refed two to three times per week with fresh growth medium and maintained at 37°C in a 5% CO_2 incubator.

Construction of Recombinant Adenovirus. The recombinant adenovirus construction strategy is based on a system developed by Dr. Xavier Danthinne (O.D.260, Inc., Boise, ID). The system comprises the cloning vector, pAd1020*Sfi*dA, containing the adenoviral left ITR and packaging signal (bp 1-358) and the adenoviral genome vector, pAd288, containing the right arm of the adenoviral genome from 3,504 bp to the end with the E3 region. pAd288 was modified by inserting the *E1b* gene (including E1b TATA box, bp 1,672-3,503) to make pAd288E1b. The right end of Ad5 [from bp 35,464 (*Pac*I) to 35,938 (*Avr*II)] was cloned from pAd288 into pBKS II (Stratagene, Cedar Creek, TX). The E4 enhancer region [from bp 35,641 (*Pac*I) to 35,822 (*Avr*II)] was replaced by a synthetic multiple cloning site made by PCR. Then, PSES-E1a [from bp 468 (E1a TATA box) to 1,644] was cloned into the multiple cloning site. The modified *Pac*I/*Avr*II fragment was cloned back into pAd288E1b to make pAd288E1b-E4PSESE1a. A CMV-EGFP expression cassette was cloned into pAd1020*Sfi*dA to make pAd1020*Sfi*-dACMVEGFP, which was then digested with *Sfi*I to release CMV-EGFP together with the adenoviral left ITR and packaging signal (bp 1-358) and a kanamycin resistance gene (Kan^r). The Kan^r-ITR-EGFP-CMV fragment was then cloned into *Sfi*I-digested pAd288E1b-E4PSESE1a. The ligated DNA was transformed into *E. coli* cells, which were then plated onto an agar plate containing both ampicillin and kanamycin. Cosmid DNA was purified, digested with *Pac*I to release adenoviral genome, and transfected into HER911E4 (~80% confluency) using a Lipofectamine 2000 transfection reagent (Invitrogen) to generate the recombinant adenovirus, AdE4PSESE1a. The total length of the recombinant viral genome is 37,821 bp. Its structure is illustrated in Fig. 1. The CMV-EGFP expression cassette in the viral genome allows us to monitor the viral propagation *in vitro* and distribution of the virus *in vivo* because enhanced green fluorescent protein (EGFP), as a marker of viral infection, can infer viral replication indirectly. The plate was incubated at 37°C under 5% CO_2 for 7 to 10 days after transfection to allow for sufficient cytopathic effect. Then AdE4PSESE1a was amplified in HER911E4 from one P60 dish to one T75 flask, to triple-flasks, and finally to cell factories. The adenovirus was purified by CsCl

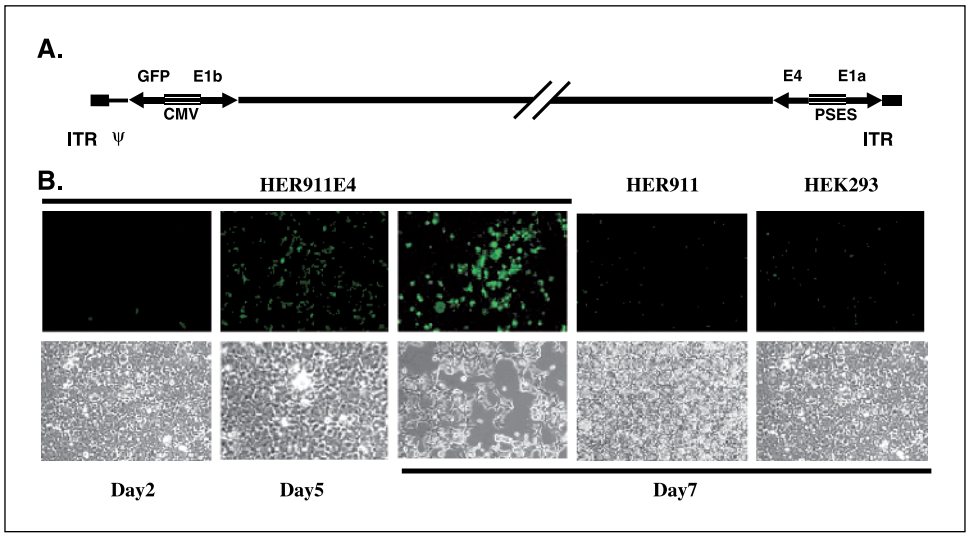

Figure 1. *A,* structure of AdE4PSESE1a. Adenoviral *E1a* gene was placed at the right end of the adenoviral genome to avoid potential interference from the adenoviral packaging signal. PSES is employed to direct the expression of *E1a* and *E4* genes. A CMV promoter-controlled EGFP expression cassette is cloned into the left end of the adenoviral genome to allow the tracking of intratumoral adenovirus. *B,* generation of AdE4PSESE1a. The viral genome was released from the cloning vector by *Pac*I and transfected into helper cells, HEK293, HER911, and HER911E4, using Lipofectamine 2000 transfection reagent. Green fluorescent cells were observed daily until the formation of plaques seen by fluorescence microscopy. The cells were observed until cytopathic effect formation under light microscopy.

gradient centrifugation. All gradient-purified viral stocks were then dialyzed against dialysis buffer (1,000 mL dialysis buffer contains 789 mL double-distilled water, 1 mL 1 mol/L $MgCl_2$, 10 mL 1 mol/L Tris-HCl (pH 7.5), and 200 mL 50% glycerol) for 24 hours at 4°C, with three buffer changes. Aliquots of purified and dialyzed viruses were stored at −70°C for future use. The viral titer was determined by Adeno-XTM Rapid Titer System (Invitrogen) according to the instructions of the manufacturer. This kit detects the adenovirus capsid hexon protein by immunohistochemistry. Final titer was expressed as infection forming units (IFU). The viral DNA was purified by phenol/chloroform extraction and was used as a template for PCR. Four PCR primers were chosen within the E4-PSES-E1a gene cassette including E4 reverse (primer 1: ACCACTCGAGCCTAGGCAAAA-TAGCACCCT), PSES reverse (primer 2: AGTACTCCGATGACGTAAAATAGT-CATAT), PSES forward (primer 3: GGAGGAACATATTGTTATTCGA), and E1a reverse (primer 4: CGGGAAAAATCTGCGAAACC). PCR was done with an initial denaturation step of 94°C for 2 minutes, followed by 35 cycles of denaturation at 94°C for 30 seconds, annealing at 50°C for 30 seconds, and extension at 72°C for 1 minute, with extension in the last cycle lasting for 10 minutes. The PCR products were analyzed on a 1% agarose gel by electrophoresis.

Adenoviral Infectivity Assay. C4-2, CWR22rv, PC-3, DU145, HeLa, LoVo, MCF10A, and HEK293 cells were seeded (2.5×10^5 cells per well) in a 12-well plate 1 day before viral infection. Cells were infected with serial doses of AdCMV-Luc (an E1/E3-deleted recombinant adenovirus carrying the luciferase reporter gene controlled by CMV promoter) from 0.05 to 37.25 multiplicity of infection (1 multiplicity of infection = 1 IFU per cell). The media were changed 24 hours after addition of the virus. The cells were harvested 48 hours after infection for luciferase assay (Promega, Madison, WI). The luciferase activities obtained were used as a reference to adjust the virus titer for each cell line to obtain a similar infectivity for the experiments. The accuracy of the above titer assay was checked by reinfecting cells with the amount of virus derived from the assay.

Western Blot Analysis. C4-2, CWR22rv, PC-3, DU145, HeLa, LoVo, and MCF10A cells were seeded in six-well plates and infected with AdE4PSESE1a and a wild-type adenovirus (Ad-wt) 1 day after cell seeding. Each cell line was infected with different amounts of virus according to the luciferase activity obtained above to achieve similar infectivities. The cells were washed with cold PBS and lysed with radioimmunoprecipitation assay buffer [1 mL modified radioimmunoprecipitation buffer supplemented with 2.5 μL proteinase inhibitors (Sigma) and 20 μL 57 mmol/L phenylmethylsulfonyl fluoride] 24 hours after infection. Cells were collected into Eppendorf tubes and incubated on ice for 1 hour. Cell debris was spun down and the supernatant was kept at −70°C. Protein concentration was evaluated by the Bradford protein assay. The same amount of protein (5 μg) collected above was subjected to SDS-PAGE separation and electroblotted to a nitrocellular membrane using a NOVEX gel system (Invitrogen). SeeBlue marker (Invitrogen) was used as a molecular weight indicator. The membrane was probed with an anti-adenovirus-5 E1a antibody (BD Biosciences PharMingen, San Diego, CA), followed by a horseradish peroxidase-conjugated anti-mouse immunoglobulin G secondary antibody (Santa Cruz Biotechnology, Inc., Santa Cruz, CA). Supersignal West Pico Chemiluminescent Substrate (Pierce, Rockford, IL) was used to detect the signal.

Reverse Transcription-PCR for E4 mRNA. CWR22rv, C4-2, PC-3, DU145, HeLa, LoVo, and MCF10A cells were seeded in P100 dishes (5×10^6 cells per dish) and infected with AdE4PSESE1a and Ad-wt 1 day after cell seeding (~80% cell confluency). Each cell line was infected with different doses of virus to achieve comparable infectivity as described above. Cells were washed once with cold PBS and lysed for RNA isolation using TRIzol reagent (Invitrogen). Cell lysates were scraped, collected in a 1.5 mL Eppendorf tube, pipetted up-down several times, and extracted with 200 mL chloroform. The aqueous phase was removed to a new Eppendorf tube and the mRNA was precipitated with isopropanol. Final total mRNA was dissolved in 30 μL diethyl pyrocarbonate-treated H_2O and its concentration was measured at A_{260}. Potential contamination of genomic DNA was checked by PCR using no reverse transcriptase as control. The RNeasy Mini kit (Qiagen, Valencia, CA) was used to purify mRNA if DNA contamination was identified. Reverse transcription-PCR was done using a kit from Invitrogen. The PCR products were analyzed on a 1% agarose gel by electrophoresis. -Actin expression by reverse transcription-PCR was used as an internal standard of RNA loading in each sample.

Viral Replication Assay. C4-2, CWR22rv, PC-3, DU145, HeLa, LoVo, MCF10A, and HEK293 cells were seeded in six-well plates (1×10^6 cells per well) 1 day before viral infection and subsequently infected with AdE4PSESE1a or Ad-wt. Each cell line was infected with standardized doses of virus as described above. The media were changed 24 hours later, and the viral supernatants were harvested 3 days after the infection. The cells were examined under the microscope daily for up to 5 days. Then, the titers of the harvested virus soups were checked by titer assay. HER911E4 cells were seeded in 96-well plates (5×10^3 cells per well) 1 day before viral infection. The cells were infected with serial volume dilutions of the harvested supernatants, ranging from 1 to 10^{-11} μL per well. A row of eight wells was used for each dose. The media were changed on day 4, and the cells were examined under the microscope on day 7. The doses of the produced viruses were shown as an LD_{50} value (the dilution factor that causes a cytopathic effect in at least four wells of cells in a row on a 96-well plate on day 7). A tissue-specificity index was obtained by dividing the LD_{50} value of therapeutic viruses to that of wild-type.

Cell Killing Assay. C4-2, CWR22rv, PC-3, DU145, HeLa, LoVo, MCF10A, and HEK293 cells were seeded in 96-well plates (5×10^3 cells per well) 1 day before infection. The cells were infected with serial doses, ranging from 50 to 5×10^{-9} multiplicity of infection of AdE4PSESE1a and Ad-wt. A row of eight wells was used for each dose. The media were changed on day 4, and the cells were examined under a light microscope on day 7. The viral killing activity was represented as an LD_{50} value. A killing activity index was obtained by dividing the LD_{50} value of therapeutic viruses to that of wild-type. The value is expressed as a $\log_{10}$ scale, such that a value of 0 indicates the therapeutic virus has the same killing activity as wild-type virus toward a cell line. A value of −1 indicates the therapeutic virus has 10 times less killing activity than wild-type virus toward a cell line.

Animal Experiments. All animal methods and procedures were approved by the Indiana University School of Medicine Institutional Animal Care and Use Committee (IACUC). CWR22rv mouse tumors were established by injecting 4×10^6 cells s.c. in the flanks of athymic nude mice (6 weeks old, males). The injected mice were castrated 3 days after cellular injection. Mice with similar tumor sizes were randomized 3 weeks after injection (nine tumors from six mice for each group) and treated with 2×10^7 IFU of either AdE4PSESE1a or AdCMV-EGFP (a replication-deficient adenovirus used as a negative control) in 100 μL 1× PBS via intratumoral injections. In addition, seven tumors from six mice were treated with 5×10^7 IFU of AdE4PSESE1a in 50 μL 1× PBS via tail vein injection. Tumor appearance and tumor size were measured once every week with calipers, and the following formula was applied to calculate tumor volume: length × width^2 × 0.5236 (23). Tumor growth curves were drawn according to the weekly measurement. Data are expressed as fold-increase in tumor size, obtained by assessing tumor size relative to the initial size at the time of virus or vehicle injection. Significant differences between treatment and control groups were analyzed using Student's t test.

Fluorescent Imaging. We used a Berthold LB981 NightOwl System (EG&G Berthold, Bad Wildbad, Germany) to monitor the expression of EGFP in AdE4PSESE1a- or AdCMV-GFP-treated tumors. The Berthold LB981 NightOwl System is an optical imager used for the measurement of or near-IR emitting molecules. It contains a Peltier cooled backlit CCD camera (576 × 385 pixels) housed within a light-tight enclosure. The excitation source is filtered using an HQ 470 bandpass filter (Chroma Technology Corp., Rockingham, VT) and uniformly illuminates the field of view of the mouse. The emission spectrum is filtered using an HQ 525 bandpass filter (Chroma Technology) to enhance the GFP fluorescence relative to the autofluorescence signal from endogenous tissue. The fluorescent images of the tumor were taken immediately and on days 3, 7, 14, 21, and 28 post-viral injections. The mice were sedated (1.5 mg/kg acepromazine and torbugesic by i.m. injection), positioned in the light-tight

chamber, and imaged with an exposure time of 100 ms. The change in fluorescent signal was depicted on a graph.

Histology and Immunohistochemistry. Tumors were removed, immediately fixed in formalin, and embedded in paraffin. Four-micrometer sections were cut into histologic sections, stained with H&E, and examined under a light microscope. For immunohistochemistry, tumor sections were deparaffinized using a sequential protocol of xylene and hydrated with graded ethanol and distilled water. All markers were determined after antigen retrieval (sample boiled for 4 minutes in a 0.01 mol/L sodium citrate buffer in a microwave oven and cooled to room temperature). After rinsing with distilled water, slides were immersed in 3% hydrogen peroxide for 20 minutes at room temperature to quench endogenous peroxidase activity. The slides were rinsed with distilled water, washed twice with PBS for 3 minutes, and blocked with superblock (Scytek Laboratories, Burlingame, CA) in a humidified chamber for 60 minutes at room temperature. After rinsing with PBS, the slides were blocked with avidin from an avidin-biotin kit (Vector Laboratories, Inc., Burlingame, CA) for 15 minutes, washed with PBS, and blocked with biotin in a humidified chamber for 15 minutes at room temperature. A rabbit polyclonal antibody to adenovirus 5 (Abcam, Cambridge, MA) was applied to slides at a dilution of 1:200. Normal rabbit immunoglobulin G was used as a control. The slides were reacted with primary antibodies overnight in humidified chambers at 4°C. After being rinsed once with PBS, a biotinylated polyclonal anti-rabbit antibody was applied to slides at a dilution of 1:500 and incubated for 1 hour. After washing with PBS, slides were incubated with avidin-biotin-peroxidase complex (Vector Laboratories) for 1 hour, washed once with PBS, stained with freshly prepared 3,3′-diaminobenzidine solution for 15 minutes, and counterstained with hematoxylin.

***In situ* Terminal Deoxynucleotidyl Transferase–Mediated Nick End Labeling Assay.** The *in situ* apoptosis detection kit was purchased from Roche Diagnostics (Indianapolis, IN). Tumor tissue sections were deparaffinized using a sequential xylene protocol and rehydrated through gradients of ethanol and distilled water. Slides were treated with 10 mmol/L Tris solution containing 1 μg/mL proteinase K for 15 minutes. All slides were rinsed thrice with PBS and incubated with 100 μL terminal deoxynucleotidyl transferase–mediated nick end labeling (TUNEL) reaction mixture (or 100 μL control labeling solution for negative control) in a humid chamber at 37°C for 30 minutes. The slides were washed thrice with PBS and incubated with 100 μL TUNEL POD solution in a humid chamber at 37°C for 30 minutes. After washing with PBS, the slides were stained with freshly prepared 3,3′-diaminobenzidine solution for 10 minutes, rinsed with PBS, and counterstained with hematoxylin.

Results

PSES Restricted the Expression of *E4* Gene in HEK293 and HER911, Thus Controlling Adenoviral Replication. To control adenoviral replication in a prostate-specific manner, we developed a new strategy to produce a TRRA. This new strategy, illustrated in Fig. 1*A*, places the adenoviral *E1a* gene at the right end of the adenoviral genome to avoid potential interference from the adenoviral packaging signal and places the prostate-specific enhancer, PSES, between *E1a* and *E4* genes to direct their expression. A CMV promoter-controlled EGFP expression cassette is cloned at the left end of the adenoviral genome to allow the monitoring of viral propagation *in vitro* and virus distribution *in vivo.* The viral genome was released from the cloning vector by restriction enzyme *Pac*I digestion and transfected into helper cells, HEK293, HER911, and HER911E4. Green fluorescent cells could be seen under the inverted fluorescent microscope on the day following transfection in all three cell lines (data not shown). For HER911E4, which expresses adenoviral E1a and E4 proteins, the number of green fluorescent cells increased with time and formed comet-like plaques 7 days after transfection; at the same time, cytopathic effect could be detected under a light microscope. For HEK293 and HER911 helper cells, which only express adenoviral E1 proteins, the quantity and brightness of green fluorescent cells did not change significantly with time (Fig. 1*B*). Under a light microscope, the appearance of cells was normal and no cytopathic effect could be detected up to 7 days after transfection. This result showed that E4 was under the tight control of PSES enhancer, which was not active in HEK293 and HER911 cells.

The gene structure of AdE4PSESE1a produced in HER911E4 was confirmed by PCR using genome DNA extracted from AdE4PSESE1a-infected cells. As shown in Fig. 2, use of E4 reverse (primer 1) and PSES reverse (primer 3) primers amplified an expected DNA fragment size of 545 bp, whereas E4 reverse (primer 1) and PSES forward (primer 2) primers did not produce a PCR product because they face the same direction. In addition, a combination of PSES forward (primer 2) and E1a reverse (primer 4) primers produced an expected DNA fragment size of 699 bp, whereas PSES reverse (primer 3) and E1a reverse (primer 4) did not produce a PCR product because they face the same direction. The above results showed that no gross rearrangement of the inserted gene occurred during virus production. AdE4PSESE1a was then amplified in HER911E4, purified by CsCl gradient method, and titered (see Materials and Methods).

Differential Adenoviral Infection Susceptibility. Because of every cell line expressing different amounts of Coxsackie-adenovirus receptor for adenovirus, their adenoviral infectivities were expected to vary. Therefore, it is necessary to establish individual infection conditions for each cell line to achieve similar infectivity among cell lines (24). We conducted an experiment to normalize the susceptibility of tumor cell lines to adenoviral infection using AdCMV-Luc, an E1/E3-deleted replication-deficient adenovirus that carries a luciferase reporter gene under the control of CMV promoter. Figure 3*A* illustrates the various viral doses required for similar infectivity in C4-2, CWR22rv, PC-3, DU145, HeLa, LoVo, MCF10A, and HEK293. For example, C4-2 was infected with 20 virus particles per cell to test whether the different viral doses shown in Fig. 3*A* for each cell result in similar luciferase activity. The cells indicated above were infected with AdCMV-Luc for 48 hours, followed by luciferase assay. As shown in Fig. 3*B*, a similar luciferase activity (about 10^5 luciferase units) could be obtained among cell lines when adenoviral

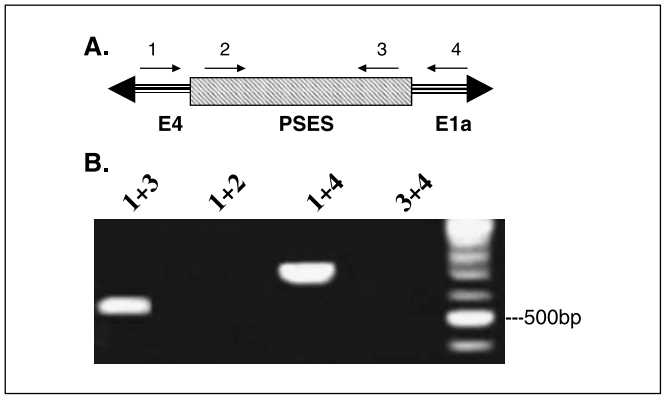

Figure 2. Confirmation of the gene structure of AdE4PSESE1a. The viral genome DNA produced in AdE4PSESE1a-infected HER911E4 was extracted by the phenol/chloroform method and used as a template for PCR. *A,* E4-PSES-E1a expression cassette in the right end of AdE4PSESE1a. *Arrows,* selected primers; E4-reverse (*1*), PSES-forward (*2*), PSES-reverse (*3*), and E1a-reverse (*4*). *B,* PCR results with the different primer pairs.

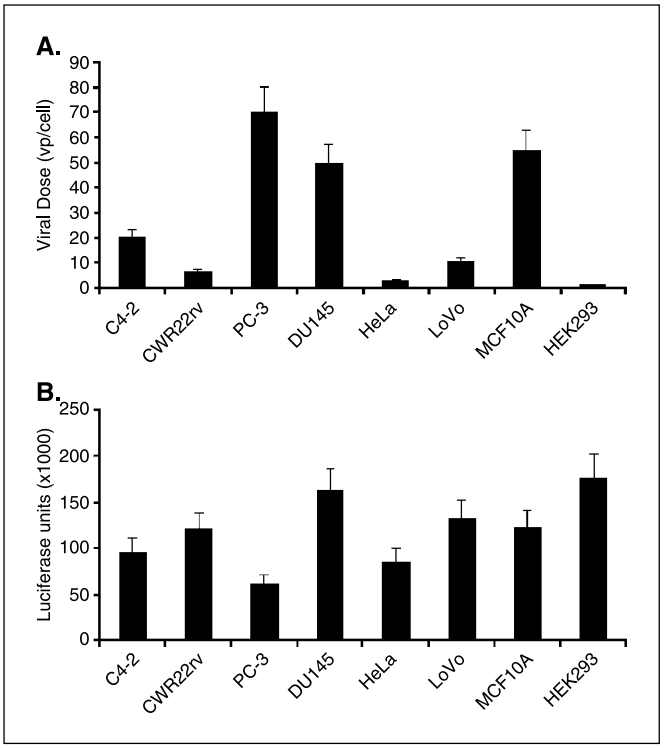

Figure 3. Standardization of infectivity in various cell lines. C4-2, CWR22rv, PC-3, DU145, HeLa, LoVo, MCF10A, and HEK293 cells were seeded (2.5×10^5 cells per well) in a 12-well plate 1 day before viral infection. Cells were infected with serial doses of AdCMV-Luc from 0.05 to 37.25 multiplicity of infection. The media were changed 24 hours after addition of the virus. The cells were harvested 48 hours after infection for luciferase assay. *A,* different viral doses required for similar infectivity in all cell lines. *B,* similar luciferase activity was obtained among cell lines when adenoviral infectivities were standardized.

infectivities were standardized. This result was applied to all subsequent *in vitro* experiments.

AdE4PSESE1a Directed the Expression of E1a and E4 in PSA/PSMA-Positive Prostate Cancer Cells. To test whether PSES enhancer could control E1a protein expression in PSA/PSMA-positive prostate cancer cells, we infected C4-2 and CWR22rv (PSA/PSMA-positive, androgen-independent prostate cancer cells) and PC-3, DU145, HeLa, LoVo, and MCF10A (PSA/PSMA-negative cells) with either AdE4PSESE1a or Ad-wt. Owing to adenoviral replication efficiency varying with each cell line, Ad-wt was used as a control for similar infectivities. Figure 4*A* depicts the ability of Ad-wt to direct E1a protein expression in all seven cell lines tested. On the other hand, AdE4PSESE1a directed E1a protein expression only in PSA/PSMA-positive prostate cancer cells, C4-2, and CWR22rv. E1a protein expression in PSA/PSMA-negative cells was undetectable or very low. Due to the lack of accessibility to E4-specific antibodies, reverse transcription-PCR was done to compare the expression profiles of E4 mRNA among several human prostate cancer cells and nonprostatic cancerous and normal cells. Figure 4*B* shows that AdE4PSESE1a expressed high amounts of E4 mRNA only in PSA/PSMA-positive prostate cancer CWR22rv and C4-2, but not in PSA/PSMA-negative PC-3, DU145, HeLa, LoVo, and MCF10A. These results not only showed that PSES retained its prostate specificity in AdE4PSESE1a but also indicated that a single enhancer core could be used to control the expression of two groups of viral genes in a bidirectional manner.

AdE4PSESE1a Propagated Selectively in PSA/PSMA-Positive Prostate Cancer Cells but Not in PSA/PSMA-Negative Cancer Cells. We did an *in vitro* viral replication assay to compare the viral replication efficiency of AdE4PSESE1a and Ad-wt. This would also determine whether AdE4PSESE1a could replicate selectively in the PSA/PSMA-positive prostate cancer cells. Cells were infected with AdE4PSESE1a or Ad-wt and the media were changed 24 hours post viral infection. The supernatants were harvested for titer assay 2 days after the medium change. Viral titer for AdE4PSESE1a was normalized by one for Ad-wt and values were represented as $\log_{10}$ phase. As shown in Table 1, AdE4PSESE1a propagated as efficiently as Ad-wt in PSA/PSMA-positive C4-2 and CWR22rv. On the other hand, AdE4PSESE1a showed a limited replication activity in PSA/PSMA-negative cells. Compared to Ad-wt, it produced 100-fold fewer viruses in LoVo, 500-fold fewer viruses in DU145, HeLa, and HEK293, 1,000-fold fewer viruses in PC-3, and 5,000-fold fewer viruses in MCF10A cells.

We conducted another experiment to investigate the tissue-restricted replication of AdE4PSESE1a. PSA/PSMA-positive and PSA/PSMA-negative cells were infected with AdE4PSESE1a and monitored daily under a fluorescent microscope up to 5 days. EGFP expression represented AdE4PSESE1a infection. At 1 day after infection, EGFP-expressing cells were easily detected in all cell types tested (Fig. 5). The number and intensity of green cells increased in PSA/PSMA-positive prostate cancer cells but not in PSA/PSMA-negative cells. At day 5, a comet-like patch of green cells had formed only in PSA/PSMA-positive prostate cancer cells. At the same time, we could detect virus plaques under a light

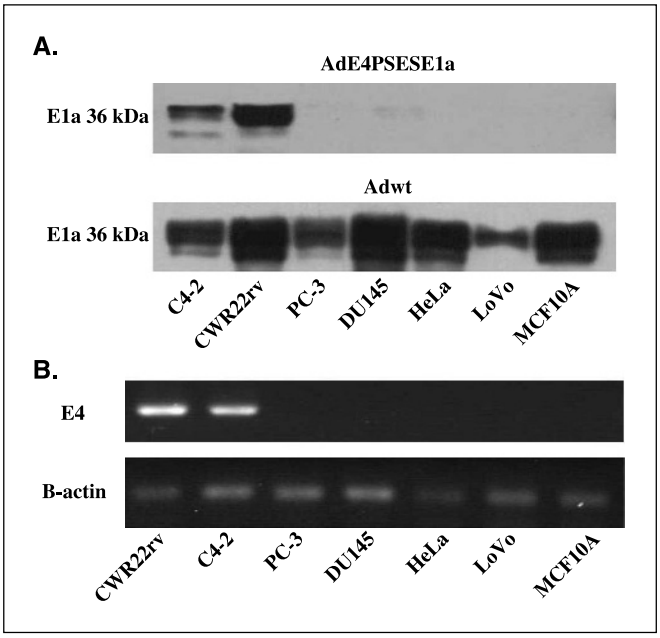

Figure 4. AdE4PSESE1a-directed E1a and E4 expression in human prostate cancer cell lines. *A,* E1a protein expression. C4-2, CWR22rv, PC-3, DU145, HeLa, LoVo, and MCF10A cells were infected with standardized doses of either AdE4PSESE1a or Ad-wt and harvested for protein preparation 24 hours postinfection. E1a protein was detected by Western blot and probed with a polyclonal antibody to Ad5 E1a protein. Ad-wt was used as a control. *B,* E4 mRNA accumulation. C4-2, CWR22rv, PC-3, DU145, HeLa, LoVo, and MCF10A cells were infected with AdE4PSESE1a and total RNA was prepared for reverse transcription-PCR 24 hours postinfection. β-Actin was used as an internal standard of RNA loading in each sample.

Table 1. Tissue/tumor-specific replication ability of AdE4PSESE1a

Cell lines	Input doses* (IFU)	Output viral doses (LD_{50} ‡)		
		AdE4	Adwt	AdE4/Adwt
C4-2	6.6×10^4	10^6	10^6	1
CWR22rv	2×10^4	10^6	10^6	1
PC-3	2.3×10^5	10^2	10^5	10^{-3}
DU145	1.6×10^5	5×10^2	10^5	5×10^{-3}
HeLa	8×10^3	5×10^3	10^6	5×10^{-3}
LoVo	3.3×10^4	10^4	10^6	10^{-2}
MCF10A	1.8×10^5	5×10^2	10^6	5×10^{-4}
HEK293	3.3×10^3	5×10^2	10^5	5×10^{-3}

Cells were seeded and infected with AdE4PSESE1a, and the supernatants were harvested for titer assay as described in Materials and Methods.
*Input viral doses mean the virus doses used to infect cells.
† Output viral doses mean the titered virus doses in titer assay.
‡ The virus production was expressed as a LD_{50} value (the dilution factor that caused a cytopathic effect in at least 4 wells of cells in a row on a 96-well plate on day 7).

microscope. All these results showed that the replication of AdE4PSESE1a is tightly controlled by PSES and restricted to PSA/PSMA-positive cells.

AdE4PSESE1a Showed Specific Cell Killing Ability in PSA/PSMA-Positive Cancer Cells. To test the tissue/tumor-specific killing activity of AdE4PSESE1a, serial dilutions of AdE4PSESE1a and Ad-wt were applied to C4-2, CWR22rv, PC-3, DU145, HeLa, LoVo, A549, MCF10A, and HEK293 in 96-well plates. Cells were monitored under the microscope daily. Figure 6 presents the viral doses that cause a cytopathic effect in at least four wells of cells in a line of 96-well plates used for each dose. AdE4PSESE1a was able to kill C4-2 and CWR22rv at the same doses as Ad-wt. On the other hand, AdE4PSESE1a required 100-fold more viruses than Ad-wt to kill LoVo, 500-fold more viruses to kill DU145 and HeLa, 1,000-fold more viruses to kill PC-3, and MCF10A, and 10,000-fold more viruses to kill HEK293 cells. This result indicates that the killing activity for AdE4PSESE1a was the same as for Ad-wt in PSA/PSMA-positive cancer cells and significantly attenuated in PSA/PSMA-negative prostate cancer cells and nonprostatic cancer cells.

AdE4PSESE1a Was Effective against the Growth of Androgen-Independent CWR22rv Prostate Tumors. CWR22rv s.c. tumors were established in athymic nude mice as described in Materials and Methods. The mice were castrated 3 days after CWR22rv inoculation to test whether AdE4PSESE1a was able to eliminate androgen-independent tumors in a castrated host. Mice were randomized 3 weeks after cell inoculation (nine tumors from six mice in each group) and received intratumoral injections of 2×10^7 IFU AdE4PSESE1a or AdCMV-GFP. A replication deficient adenovirus was used as a negative control. In addition, seven tumors from six mice were treated i.v. with 5×10^7 IFU of AdE4PSESE1a in 50 μL 1× PBS at 1-week intervals. Tumor sizes were monitored once a week. Figure 7*A* shows that tumor growth was significantly retarded in the AdE4PSESE1a-treated groups regardless of the route of viral injection compared with those in the AdCMV-GFP-treated group. Two tumors from two animals disappeared in the AdE4PSESE1a intratumoral injection group (Fig. 7*A*). Three tumors from three different animals disappeared in the tail-vein injection group (Fig. 7*C*). When tumors from the intratumoral injection group

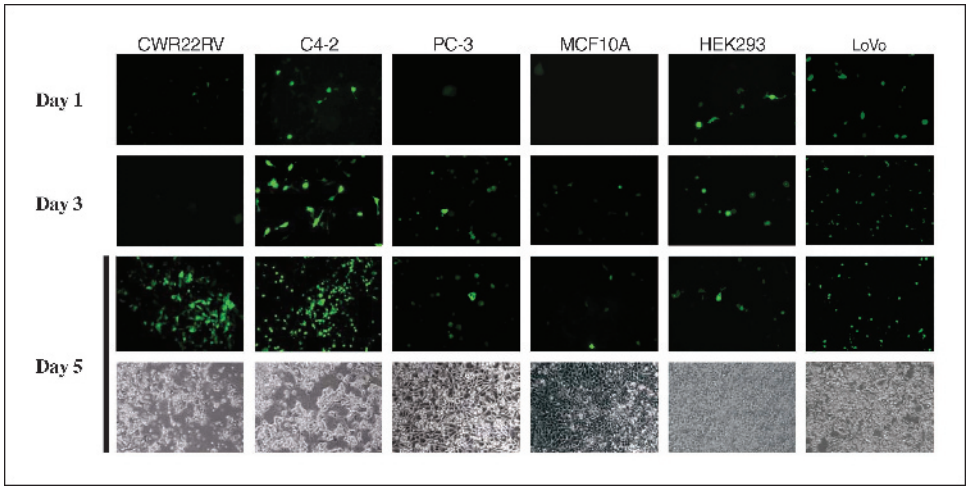

Figure 5. Tissue/tumor-specific replication ability of AdE4PSESE1a. CWR22rv, C4-2, PC3, MCF10A, and HEK293 cells were infected with standardized doses of AdE4PSESE1a and monitored daily under fluorescent microscopy and light microscopy up to 5 days after viral infection. EGFP expression represented AdE4PSESE1a infection (×20).

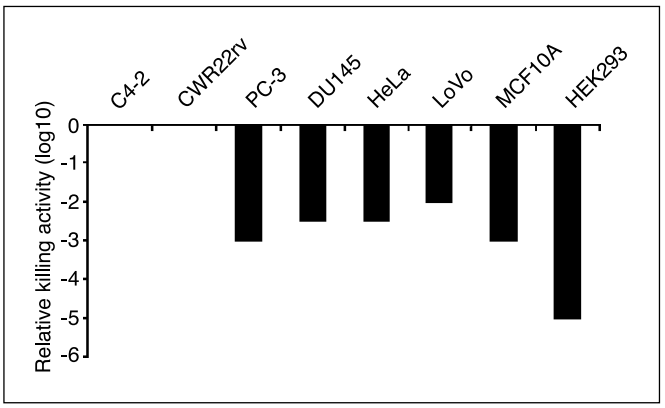

Figure 6. Tissue/tumor-specific killing activity of AdE4PSESE1a. Serial dilutions of AdE4PSESE1a and Ad-wt were applied to C4-2, CWR22rv, PC-3, DU145, HeLa, LoVo, MCF10A, and HEK293 in 96-well plates. The virus doses are the same in the first row. Cells were monitored under the microscope daily. The viral killing activity was shown as an LD_{50} value. A tissue/tumor-specific killing index was obtained by dividing the LD_{50} value of therapeutic viruses to that of wild-type. The value is expressed as a $\log_{10}$ scale, such that a value of 0 indicates the therapeutic virus has the same killing activity as wild-type virus toward a cell line. A value of -1 indicates the therapeutic virus has 10 times less killing activity than wild-type virus toward a cell line.

were harvested, we observed that AdCMV-GFP- and AdE4PSESE1a-treated tumors exhibited different appearances. In the AdCMV-GFP-treated group, the tumors were big, solid, and evenly hard. On the other hand, in the AdE4PSESE1a-treated group, tumors were small with some fragmentary and necrotic cotton-shaped tissues embedded in a turbid liquid. Tumor histology revealed that small, patchy island-shaped tumor tissues were surrounded by extensive necrotic tissue inside the tumors in the AdE4PSESE1a-treated group (Fig. 8*A* and *C*). However, the periphery of the necrotic area consisted of a shallow layer of healthy tumor cells (Fig. 8*C*), suggesting that viruses did not reach the outer rim of the tumors, which were still growing actively. This phenomenon might contribute to a minor gain in tumor size in the very late phase of the animal experiments, especially in tumors treated by intratumoral injection (Fig. 7*A*). In the AdCMV-GFP-treated group, the tumor cells were healthy and evenly distributed inside the tumors with very little necrotic tissue (Fig. 8*B* and *D*). Anti-adenovirus-5 immunohistochemical staining revealed that extensive viral infection existed throughout the treated tumors, mainly in tumor cells at the border between tumor and necrosis in AdE4PSESE1a-treated tumors (Fig. 8*E*). Anti-adenovirus-5 immunohistochemical staining was absent in AdCMV-GFP-treated tumors (Fig. 8*E*).

In situ TUNEL assays were done to detect apoptotic bodies in the AdE4PSESE1a-treated tumors. Dark-brown nuclear-staining cells were found around the border between the tumor necrosis and the tumor (Fig. 8*G*), indicating that programmed cell death is involved in the process of tumor killing. No dark-brown cells could be found in either the tumor or necrotic areas (Fig. 8*H*).

Infection of AdE4PSESE1a Could Be Monitored via a Fluorescent Imaging System. AdE4PSESE1a carries EGFP under the control of CMV promoter to track its infection and distribution in animal tumors via a fluorescent imaging system. The expression of EGFP in AdE4PSESE1a-treated tumors was imaged with an LB981 Molecular Light Imager (Night OWL) system (25) at 3 to 28 days after viral injection. The EGFP signal was negative right after AdE4PSESE1a injection because the adenovirus did not express enough EGFP at that time (data not shown). AdCMV-GFP-treated tumors never showed an EGFP signal compared with background. A strong signal showed up on the images 3 days after AdE4PSESE1a injection (Fig. 9*A*), which suggests that the virus infected the tumor cells and replicated rapidly. During the following 2 weeks, fluorescence dropped slightly. Three AdE4PSESE1a-treated (intratumoral injection) tumors showed consistent, significant EGFP signals throughout the treatment period. The data for these three tumors are shown in Fig. 9*B*.

Discussion

TRRA provides an efficient *in vivo* gene delivery method that overcomes the problems encountered in the majority of gene

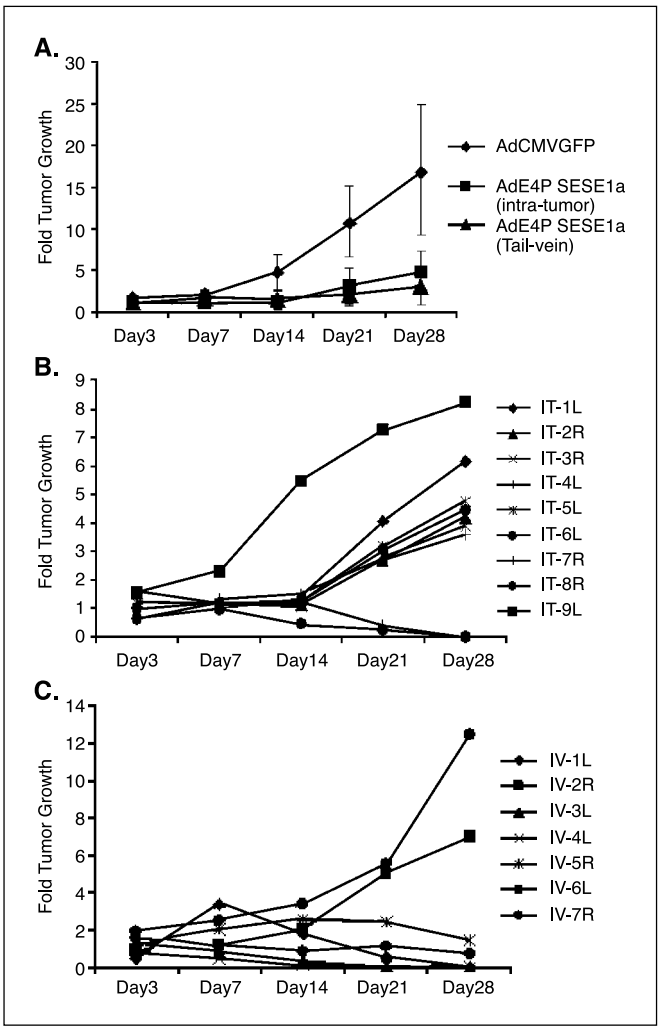

Figure 7. Evaluation of antitumor effect of AdE4PSESE1a *in vivo*. A CWR22rv prostate tumor s.c. model was established in athymic nude mice. Mice were randomized 3 weeks after cell inoculation (nine tumors from six mice in each group) and treated with 2×10^7 IFU of either AdE4PSESE1a or AdCMV-EGFP in 100 μL 1× PBS via intratumor injections. In addition, seven tumors from six mice were treated i.v. with 5×10^7 IFU of AdE4PSESE1a in 50 μL 1× PBS at 1-week intervals. Tumor sizes were monitored once every week. *A,* tumor size from each group was averaged. *B,* the sizes of tumors treated by intratumor injection were plotted individually. Two tumors from two mice disappeared in the AdE4PSESE1a intratumoral injection group. *C,* the sizes of tumors treated by i.v. injection were plotted individually. Three tumors from three mice disappeared in the tail-vein injection group.

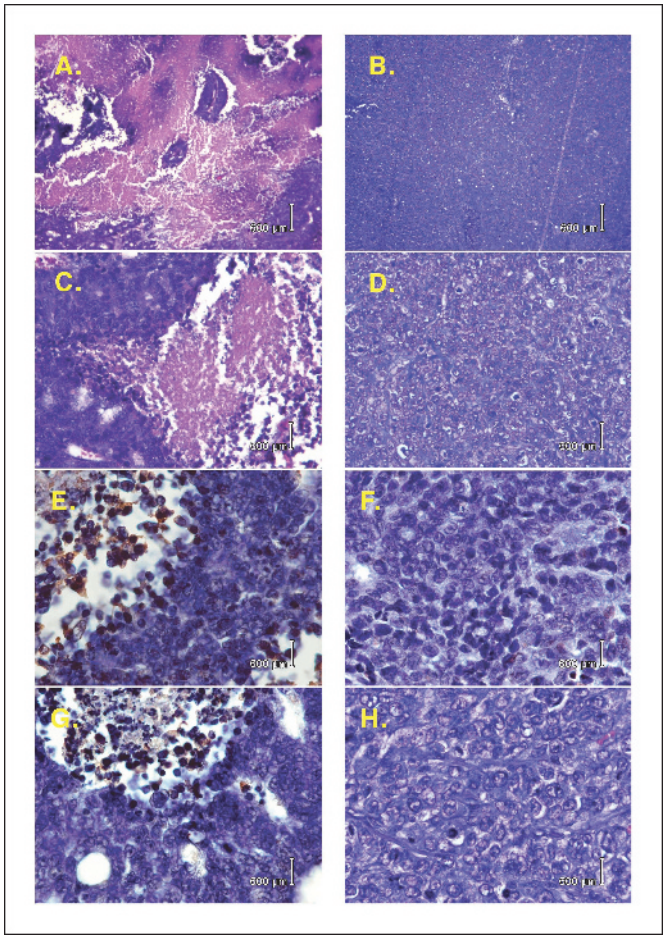

Figure 8. Histologic representations of virus-treated tumors. At 8 weeks after virus injection, tumor samples were collected for paraffin sections followed by H&E staining. Small, patchy, island-shaped tumor tissues were surrounded by extensive non-cell necrotic tissue inside the tumors in the AdE4PSESE1a-treated group (*A,* H&E ×4; *C,* H&E ×10). In the AdCMV-GFP-treated sections, very little necrotic tissue could be seen (*B,* H&E ×4; *D,* H&E ×10). Anti-adenovirus-5 immunohistochemical staining revealed that extensive viral infection exists throughout the treated tumors, mainly in tumor cells at the border between tumor and necrosis (*E,* × 20). Anti-adenovirus-5 immunohistochemical staining was absent in nontreated tumors (*F,* × 20). *In situ* TUNEL assays were done to detect apoptotic bodies in the AdE4PSESE1a-treated tumor group. Dark-brown nuclear-staining cells were found bordering the tumor necrosis and the tumor (*G,* × 20) but no dark-brown cells could be found either in the tumor or in necrosis areas (*H,* × 20).

therapy protocols. One way to construct a TRRA is by using tissue/tumor-specific promoters to control the expression of viral regulatory proteins (26, 27). There are six early transcription units in the adenovirus backbone. The first unit to be activated after entry into the nucleus is the E1a/E1b region. The adenovirus E1a proteins play important roles in the process of adenovirus gene expression and transcription (28, 29). Tissue- or tumor-specific promoters/enhancers are used to replace the E1a promoter-enhancer region, with the rationale that expression of E1a, and therefore of the whole adenovirus transcription program, will depend on these tissue- or tumor-specific promoters (30). This is the most commonly used strategy to make a TRRA. Currently, four promoters, including kallikrein 2, PSA, rat probasin, and osteocalcin, are under extensive investigation for producing prostate-restricted replicative adenovirus (2, 5, 7, 8). In our previous investigations, PSES showed high activity specifically in C4-2 and CWR22rv PSA/PSMA-positive and androgen-independent prostate cancer cells (12). A replication-deficient recombinant adenovirus carrying the luciferase reporter gene under the control of PSES enhancer drove high luciferase activity almost exclusively in PSA/PSMA-positive prostate cancer cells regardless of androgen status. We believe that PSES has several advantages over kallikrein 2 (7), PSA (2), rat probasin (31, 32), and osteocalcin promoters (3, 4). First, PSA, promoters from kallikrein 2, and rat probasin are highly androgen-dependent and may not be the best choice for patients undergoing androgen-ablation therapy. Second, probasin is a murine PSA, and the tissue-specific activity of its promoter in humans has not been extensively tested. Third, although our study of osteocalcin promoter indicates that osteocalcin promoter is active in androgen-independent cancer cells, our data also suggest that osteocalcin promoter may be active in several other organs besides bone and requires more vigorous testing to clarify its tissue specificity (33).

Early studies of E1a-based replicative-competent adenoviruses showed various degrees of success as well as certain limitations. The success of TRRA depends on the tightness of the tissue/tumor-restricted promoter/enhancer. Some promoters are highly influenced by the context of the vector backbone, resulting in leaky E1a expression and loss of specificity. Combinatorial control of Ad5 E1a and E1b, for example E1a under the control of probasin promoter and E1b under the control of PSA promoter, was shown to achieve better tissue-specific replication than control of *E1* gene expression alone (7, 8). However, it may not be easy to find two tightly controlled tissue-specific promoters for any single tumor type, such as breast cancer. Besides, juxtaposing promoters with heterogenous sequences could result in promoter competition, squelching of transcription factors, or loss of tissue specificity (34). On the other hand, juxtaposing promoters with a homologous region could result in homologous recombination and deletion of transgenes important for viral expression. Using a single promoter to drive both *E1a* and *E1b* genes could avoid homologous recombination, promoter competition, and the squelching effect of transcription factors during gene transcription (35). However, we also experienced leaky replication with this approach depending on the promoter as well as the cell line.

Besides *E1a* and *E1b* genes, the *E4* genes also play critical roles in efficient viral replication and can be controlled by a tissue/tumor-specific promoter. The adenovirus *E4* gene constitutes around 10% of the viral genome and is located at the right end of the viral genome. It encodes several regulatory proteins with pleiotropic functions. Genetic analysis has shown that E4 products are essential for productive virus infection. Removal of the E4 region severely disrupts viral gene expression in transduced cells and shows that E4 products play vital roles in viral infection. The E4 proteins are involved in several levels of regulation of cellular and viral gene expression, viral DNA replication, late viral mRNA splicing and accumulation, viral protein synthesis, host shutoff, virus assembly, E2 expression, and adeno-associated virus helper function (36–39). Several sets of differentially spliced mRNAs are generated from the E4 region during viral infection (40–43).

However, new strategies to selectively control *E4* gene expression via promoter/enhancer are still uncommon. The reason may be that E4 proteins are cytotoxic (44). However, E1a and E4 targeting may synergize each other, resulting in both a highly selective TRRA and neutralization of E4 protein

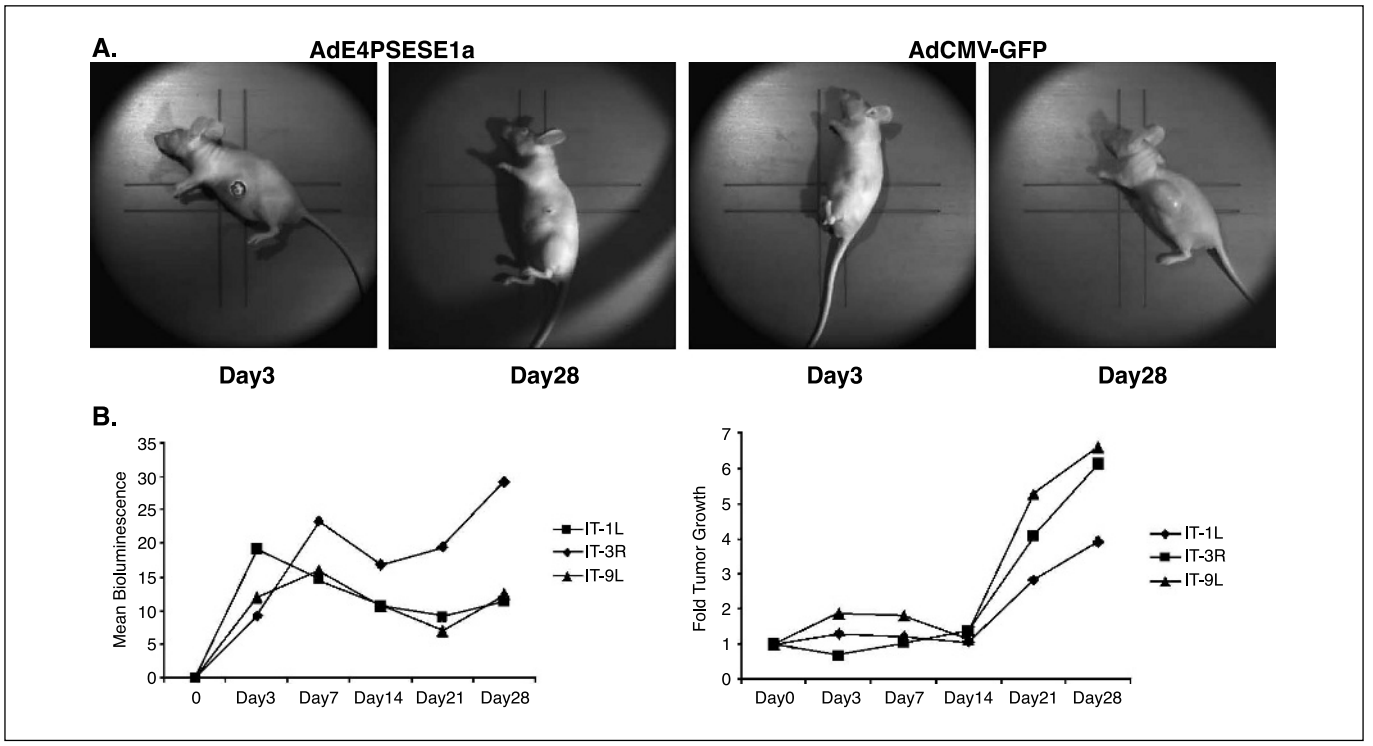

Figure 9. GFP bioluminescence and tumor size in s.c. tumor models. The LB981 Molecular Light Imager (Night OWL) system can track virus infection and distribution in animal tumor models because AdE4PSESE1a carries an EGFP. AdCMV-GFP was used as a control. *A,* bioluminescence in AdE4PSESE1a-treated or AdCMV-GFP-treated tumors. *B,* three AdE4PSESE1a-treated (intratumoral injection) tumors showed consistent, statistically significant EGFP signals throughout the treatment period.

cytotoxicity. Therefore, controlling both E1a and E4 regions by a single promoter can result in a more specific viral replication. There are several reports of successfully controlling adenoviral replication by controlling the expression of *E1a* and *E4* genes (10, 11, 30, 45). Some studies controlling adenovirus *E1a* and *E4* genes by tissue/tumor-restricted promoters have obtained high tissue/tumor-specific targeting (11, 45, 46). For example, the adenovirus mutant ONYX-411, in which the *E1a* and *E4* genes were driven by different copies of the human E2F promoter, showed a high selectively in retinoblastoma-deficient tumor cells (11). OVA002 has the *E1a* and *E4* genes under the control of E2F promoter and human telomerase promoter, respectively, and shows higher tumor selectivity than OVA001, in which E1a is driven by the E2F promoter and E4 is under its own promoter (45).

Previously we showed that PSES exhibits very restricted tissue-specific activity in PSA/PSMA-positive prostate cancer cells. In this report, we constructed a TRRA AdE4PESEE1a by inserting E1a in the right end of adenoviral genome to avoid potential interference from the adenoviral packaging signal and putting PSES between *E1a* and *E4* genes to control the expression of *E1a* and *E4* genes simultaneously. AdE4PESEE1a showed tightly controlled replication. It cannot replicate well in all nonprostatic cancer cells tested thus far, not even in HEK293 and HER911, which express E1a and E1b proteins. AdE4PESEE1a replicated as efficiently as Ad-wt in PSA/PSMA-positive cancer cells. The diminishment of AdE4PESEE1a to replicate in HEK293 and HER911 indicates the stringent requirement of E4 proteins for efficient viral replication. We detected low levels of E4 mRNA expression in PC-3 and DU145. However, AdE4PESEE1a produced 1,000-fold fewer viruses than Ad-wtin PC-3, suggesting that adenovirus requires more E4 protein expression for efficient viral replication.

AdE4PSESE1a showed better tumor suppression activity for androgen-independent prostate tumors in castrated hosts than AdCMV-GFP. In particular, two tumors disappeared in the intratumor injection group and three tumors disappeared in the tail-vein injection group. AdE4PESEE1a has another advantage over other TRRAs. It encodes a reporter, EGFP, which allows us to track the virus infection, replication, and cell killing *in vitro* continuously with a fluorescent microscope. EGFP also allows us to conduct live imaging to monitor viral infection, amplification, and distribution continuously through a CCD camera, such as the Berthold LB981 NightOwl System used in this study. Figure 9*A* depicts a dramatic increase in EGFP expression 3 days after virus injection. We believe this is due to rapid viral replication and spreading of AdE4PSESE1a, owing to AdCMV-GFP-treated tumors not exhibiting the same phenomenon. It is quite surprising that rapid viral amplification only occurred in the first few days (Fig. 9*A*) and EGFP signals started to drop 5 days after virus injection. It is not clear what reduced viral replication after the first phase of acute replication. It seems that tumor growth and death rate reached a balance in the first 2 weeks after virus injection and then tumor growth rate exceeded death rate, resulting in new tumor growth (Fig. 9*B*). The regrowth of tumor restimulated viral replication, as indicated by a slight rebound of the EGFP signal 21 days after viral injection (Fig. 9*B*). The immunohistochemistry indicated persistent viral replication (Fig. 8*E*) for 28 days after virus injection. This result is consistent with Harrison's report that

complete tumor responses to adenovirus dl309 therapy are rarely achieved despite viral persistence in the tumor (47). For a TRRA to succeed in the clinic, it is critical to understand how viral replication is slowed down after the initial acute replication phase.

In conclusion, we developed a prostate-restricted replicative adenovirus, AdE4PSESE1a, by controlling the expression of *E1a* and *E4* genes with a chimeric prostate-specific transcriptional enhancer, PSES. AdE4PSESE1a showed similar killing and replication activities to Ad-wt in PSA/PSMA-positive androgen-independent human prostate cancer cells, and much lower activities in PSA/PSMA-negative prostate cancer cells and nonprostate cancer cells. The inhibition of the growth of androgen-independent CWR22rv s.c. tumors in castrated animals indicated the therapeutic potential of AdE4PSESE1a for the treatment of androgen-independent cancers. This study revealed that adenoviral replication slowed down after several days of acute replication, a phenomenon that needs to be overcome to optimize the therapeutic use of TRRA. We believe that AdE4PSESE1a could be further improved by replacing the CMV-EGFP expression cassette with a therapeutic gene, such as an apoptosis inducer or a suicide gene controlled by a tissue specific promoter, to further enhance its therapeutic efficacy. This report also provides a new strategy to construct a TRRA for those tumor types that have limited tissue/tumor-specific promoters available.

Acknowledgments

Received 10/12/2004; revised 12/21/2004; accepted 12/29/2004.

Grant support: NIH grant CA074042 (C. Kao), DOD grant W23RX-3270-N729 (C. Kao), Phi Beta Psi Sorority Award (C. Kao), and DOD DAMD 17-03-1-0077 (T.A. Gardener).

The costs of publication of this article were defrayed in part by the payment of page charges. This article must therefore be hereby marked advertisement in accordance with 18 U.S.C. Section 1734 solely to indicate this fact.

References

1. Huggins C, Hodges CV. Studies on prostatic cancer: I. The effect of castration, of estrogen and of androgen injection on serum phosphatases in metastatic carcinoma of the prostate. 1941. J Urol 2002; 168:9–12.
2. Gotoh A, Ko SC, Shirakawa T, et al. Development of prostate-specific antigen promoter-based gene therapy for androgen-independent human prostate cancer. J Urol 1998;160:220–9.
3. Koeneman KS, Kao C, Ko SC, et al. Osteocalcin-directed gene therapy for prostate-cancer bone metastasis. World J Urol 2000;18:102–10.
4. Ko SC, Cheon J, Kao C, et al. Osteocalcin promoter-based toxic gene therapy for the treatment of osteosarcoma in experimental models. Cancer Res 1996;56:4614–9.
5. Matsubara S, Wada Y, Gardner TA, et al. Aconditional replication-competent adenoviral vector, Ad-OC-E1a, to cotarget prostate cancer and bone stroma in an experimental model of androgen-independent prostate cancer bone metastasis. Cancer Res 2001;61: 6012–9.
6. Rodriguez R, Schuur ER, Lim HY, Henderson GA, Simons JW, Henderson DR. Prostate attenuated replication competent adenovirus (ARCA) CN706: a selective cytotoxic for prostate-specific antigen-positive prostate cancer cells. Cancer Res 1997;57:2559–63.
7. Yu DC, Sakamoto GT, Henderson DR. Identification of the transcriptional regulatory sequences of human kallikrein 2 and their use in the construction of calydon virus 764, an attenuated replication competent adenovirus for prostate cancer therapy. Cancer Res 1999;59:1498–504.
8. Yu DC, Chen Y, Seng M, Dilley J, Henderson DR. The addition of adenovirus type 5 region E3 enables calydon virus 787 to eliminate distant prostate tumor xenografts. Cancer Res 1999;59:4200–3.
9. Hsieh CL, Yang L, Miao L, et al. A novel targeting modality to enhance adenoviral replication by vitamin D(3) in androgen-independent human prostate cancer cells and tumors. Cancer Res 2002;62: 3084–92.
10. Banerjee NS, Rivera AA, Wang M, et al. Analyses of melanoma-targeted oncolytic adenoviruses with tyrosinase enhancer/promoter-driven E1A, E4, or both in submerged cells and organotypic cultures. Mol Cancer Ther 2004;3:437–49.
11. Johnson L, Shen A, Boyle L, et al. Selectively replicating adenoviruses targeting deregulated E2F activity are potent, systemic antitumor agents. Cancer Cell 2002;1:325–37.
12. Lee SJ, Kim HS, Yu R, et al. Novel prostate-specific promoter derived from PSA and PSMA enhancers. Mol Ther 2002;6:415–21.
13. Graham FL. Growth of 293 cells in suspension culture. J Gen Virol 1987;68:937–40.
14. Fallaux FJ, Kranenburg O, Cramer SJ, et al. Characterization of 911: a new helper cell line for the titration and propagation of early region 1-deleted adenoviral vectors. Hum Gene Ther 1996;7:215–22.
15. He TC, Zhou S, da Costa LT, Yu J, Kinzler KW, Vogelstein B. A simplified system for generating recombinant adenoviruses. Proc Natl Acad Sci U S A 1998;95:2509–14.
16. Thalmann GN, Anezinis PE, Chang SM, et al. Androgen-independent cancer progression and bone metastasis in the LNCaP model of human prostate cancer. Cancer Res 1994;54:2577–81.
17. Tepper CG, Boucher DL, Ryan PE, et al. Characterization of a novel androgen receptor mutation in a relapsed CWR22 prostate cancer xenograft and cell line. Cancer Res 2002;62:6606–14.
18. Kaighn ME, Narayan KS, Ohnuki Y, Lechner JF, Jones LW. Establishment and characterization of a human prostatic carcinoma cell line (PC-3). Invest Urol 1979;17:16–23.
19. Stone KR, Mickey DD, Wunderli H, Mickey GH, Paulson DF. Isolation of a human prostate carcinoma cell line (DU 145). Int J Cancer 1978;21:274–81.
20. Soule HD, Maloney TM, Wolman SR, et al. Isolation and characterization of a spontaneously immortalized human breast epithelial cell line, MCF-10. Cancer Res 1990;50:6075–86.
21. Jones HW Jr, McKusick VA, Harper PS, Wuu KD. George Otto Gey. (1899-1970). The HeLa cell and a reappraisal of its origin. Obstet Gynecol 1971;38: 945–9.
22. Drewinko B, Romsdahl MM, Yang LY, Ahearn MJ, Trujillo JM. Establishment of a human carcinoembryonic antigen-producing colon adenocarcinoma cell line. Cancer Res 1976;36:467–75.
23. Gleave M, Hsieh JT, Gao CA, von Eschenbach AC, Chung LW. Acceleration of human prostate cancer growth *in vivo* by factors produced by prostate and bone fibroblasts. Cancer Res 1991;51:3753–61.
24. Steinwaerder DS, Carlson CA, Lieber A. DNA replication of first-generation adenovirus vectors in tumor cells. Hum Gene Ther 2000;11:1933–48.
25. Stanley PE. Commercially available luminometers and imaging devices for low-light level measurements and kits and reagents utilizing bioluminescence or chemiluminescence: survey update 5. J Biolumin Chemilumin 1997;12:61–78.
26. Galanis E, Vile R, Russell SJ. Delivery systems intended for *in vivo* gene therapy of cancer: targeting and replication competent viral vectors. Crit Rev Oncol Hematol 2001;38:177–92.
27. Siders WM, Halloran PJ, Fenton RG. Transcriptional targeting of recombinant adenoviruses to human and murine melanoma cells. Cancer Res 1996;56:5638–46.
28. White E. Regulation of the cell cycle and apoptosis by the oncogenes of adenovirus. Oncogene 2001;20:7836–46.
29. Jones N. Transcriptional modulation by the adenovirus *E1a* gene. Curr Top Microbiol Immunol 1995; 199:59–80.
30. Hallenbeck PL, Chang YN, Hay C, et al. A novel tumor-specific replication-restricted adenoviral vector for gene therapy of hepatocellular carcinoma. Hum Gene Ther 1999;10:1721–33.
31. Greenberg NM, DeMayo FJ, Sheppard PC, et al. The rat probasin gene promoter directs hormonally and developmentally regulated expression of a heterologous gene specifically to the prostate in transgenic mice. Mol Endocrinol 1994;8:230–9.
32. DeWeese TL, van der Poel H, Li S, et al. A phase I trial of CV706, a replication-competent, PSA selective oncolytic adenovirus, for the treatment of locally recurrent prostate cancer following radiation therapy. Cancer Res 2001;61:7464–72.
33. Jung C, Ou YC, Yeung F, Frierson HF Jr, Kao C. Osteocalcin is incompletely spliced in non-osseous tissues. Gene 2001;271:143–50.
34. Rubinchik S, Lowe S, Jia Z, Norris J, Dong J. Creation of a new transgene cloning site near the right ITR of Ad5 results in reduced enhancer interference with tissue-specific and regulatable promoters. Gene Ther 2001;8:247–53.
35. Doronin K, Kuppuswamy M, Toth K, et al. Tissue-specific, tumor-selective, replication-competent adenovirus vector for cancer gene therapy. J Virol 2001;75: 3314–24.
36. Halbert DN, Cutt JR, Shenk T. Adenovirus early region 4 encodes functions required for efficient DNA replication, late gene expression, and host cell shutoff. J Virol 1985;56:250–7.
37. Huang MM, Hearing P. Adenovirus early region 4 encodes two gene products with redundant effects in lytic infection. J Virol 1989;63:2605–15.
38. Richardson WD, Westphal H. A cascade of adenovirus early functions is required for expression of adeno-associated virus. Cell 1981;27:133–41.
39. Weinberg DH, Ketner G. Adenoviral early region 4 is required for efficient viral DNA replication and for late gene expression. J Virol 1986;57:833–8.
40. Dix I, Leppard KN. Regulated splicing of adenovirus type 5 E4 transcripts and regulated cytoplasmic accumulation of E4 mRNA. J Virol 1993;67: 3226–31.
41. Freyer GA, Katoh Y, Roberts RJ. Characterization of the major mRNAs fromadenovirus 2 early region 4 by

cDNA cloning and sequencing. Nucleic Acids Res 1984;12:3503–19.
42. Tigges MA, Raskas HJ. Splice junctions in adenovirus 2 early region 4 mRNAs: multiple splice sites produce 18 to 24 RNAs. J Virol 1984; 50:106–17.
43. Virtanen A, Gilardi P, Naslund A, LeMoullec JM, Pettersson U, Perricaudet M. mRNAs from human adenovirus 2 early region 4. J Virol 1984; 51:822–31.
44. Ji L, Bouvet M, Price RE, Roth JA, Fang B. Reduced toxicity, attenuated immunogenicity and efficient mediation of human p53 gene expression *in vivo* by an adenovirus vector with deleted E1-E3 and inactivated E4 by GAL4-TATA promoter replacement. Gene Ther 1999;6:393–402.
45. Bristol JA, Zhu M, Ji H, et al. *In vitro* and *in vivo* activities of an oncolytic adenoviral vector designed to express GM-CSF. Mol Ther 2003; 7:755–64.
46. Kirn D, Martuza RL, Zwiebel J. Replication-selective virotherapy for cancer: Biological principles, risk management and future directions. Nat Med 2001;7: 781–7.
47. Harrison D, Sauthoff H, Heitner S, Jagirdar J, Rom WN, Hay JG. Wild-type adenovirus decreases tumor xenograft growth, but despite viral persistence complete tumor responses are rarely achieved—deletion of the viral E1b-19-kD gene increases the viral oncolytic effect. Hum Gene Ther 2001;12:1323–32.

Antitumor Activity of Ad-IU-2, a Prostate-Specific Replication-Competent Adenovirus Encoding Apoptosis Inducer, TRAIL.

Juan Antonio Jiménez[1,2,3], Xiong Li[1,3], Yan-Ping Zhang[1,3], Kyung Hee Bae[1,3], Pankita Pandya[1], Yousef Mohammadi[1,3], Chinghai Kao[1,2,3], and Thomas A. Gardner[1,2,3]

Authors' Affiliations: *[1]Department of Urology; [2]Department of Microbiology and Immunology, [3]Walther Oncology Center; Indiana University School of Medicine, Indianapolis, Indiana.*

Grant Support: NIH F31 CA106215-01 (J.A. Jiménez), DOD DAMD 17-03-1-0077 (T.A. Gardner), NIH R01 CA074042 (C. Kao), and DOD W23RX-3270-N729 (C. Kao).

Requests for Reprints: Chinghai Kao, Department of Urology, Indiana University School of Medicine, 1001 West 10th Street, OPW320, Indianapolis, IN 46202. Phone: (317) 278-6873; Fax: (317) 278-3432; E-mail: chkao@iupui.edu.

Abstract

In 2006, it is estimated that prostate cancer will account for the most new cancer diagnoses, aside from skin cancer, at 234,460 men in the United States and will be the second most common cause of cancer deaths at 27,350 men. Currently, 25% of men treated for localized prostate cancer will experience biochemical disease recurrence within ten years of treatment, and all recurrent tumors become refractory to hormone therapy. Here, we investigate the antitumor effect of tumor necrosis factor-related apoptosis-inducing ligand (TRAIL) delivered by Ad-IU-2, a prostate-specific replication-competent adenovirus (PSRCA), against androgen-independent prostate cancer. Ad-IU-2 was made by placing adenoviral *E1a* and *E4* genes under the control of the bidirectional chimeric enhancer prostate-specific enhancing sequence (PSES) upstream from the right ITR as well as *E1b* and membrane-bound TRAIL cDNA under the control of PSES downstream of the left ITR. Expression of early adenoviral genes and TRAIL was limited to prostate-specific antigen (PSA) and prostate-specific membrane antigen (PSMA)-positive cells. Furthermore, Ad-IU-2 induced apoptosis specifically in PSA/PSMA-positive cells above that induced by a PSRCA. Likewise, the tumor cell killing activity was two-fold greater than that of a PSRCA. The growth of subcutaneous androgen-independent CWR22rv tumors in the flanks of athymic nude mice was inhibited following intralesional injection of Ad-IU-2. TRAIL-mediated bystander killing of adjacent PSA/PSMA-negative PC-3 cells was observed and augments the killing power of a PSRCA. Ad-IU-2 is an effective molecular therapeutic for androgen-independent prostate cancer due to its strong tissue-specificity and powerful TRAIL-mediated antitumor activity and bystander killing effect.

Introduction

In 2005, it is estimated that prostate cancer will account for the most new cancer diagnoses, aside from skin cancer, at 234,460 men in the United States and will be the second most common cause of cancer deaths at 27,350 men (1). Current therapies for men presenting with localized prostate cancer include radical prostatectomy, cryoablation therapy, external beam radiation and brachytherapy; however, 25% of these men will experience biochemical disease recurrence within ten years of treatment (2, 3). Furthermore, up to 9% of patients will be diagnosed with metastatic disease at initial presentation (1). In men with locally advanced and distant metastatic prostate cancer, current treatment approaches are merely palliative. In these patients, androgen ablation therapy slows the dissemination of the disease but, once the cancer changes its androgen status, tumors become refractory to hormonal treatment. Suppression of serum prostate-specific antigen (PSA) levels is observed in only 85% of cases, with PSA rebounds occurring in 12 to 24 months (4). Results from phase III clinical studies have recently suggested a role for docetaxel in the treatment of androgen-independent prostate cancer, demonstrating a two month survival advantage in addition to palliation (5, 6). Unfortunately, dose-limiting toxicities associated with such chemotherapies limit the amount of the drug that can be delivered to the tumor, allowing the cancer to survive and fail therapy. Due to the limitations of current treatment modalities, there exists an urgent need to develop novel therapies to target both organ-confined and metastatic prostate cancer.

Tumor necrosis factor-related apoptosis-inducing ligand (TRAIL), also known as Apo-2 ligand, is a member of the tumor necrosis factor (TNF) family and has been shown to preferentially kill tumor cells over normal cells. Originally discovered because of its similarity to Fas-ligand, TRAIL is a 32 kDa type II transmembrane protein, whose C-terminal extracellular

domain (amino acids 114-281) is homologous with other members of the TNF family (7, 8). TRAIL induces apoptosis by binding to the death domain-containing receptors DR4 and DR5; however, the death signal is not transduced via the adaptor molecule FADD. Instead, the death protease FLICE2 is believed to be engaged which cleaves the initiating caspase 8 to begin the caspase cascade (9). The selectivity of TRAIL for cancer cells over normal cells makes it a prime candidate for anticancer therapy. TRAIL expression has been detected in several normal human tissues which suggests that TRAIL is not toxic to those cells *in vivo* (10). In essence, these cells are protected from the apoptotic effects of TRAIL by an antagonistic decoy receptor, TRID, which lacks an intracellular domain and is found on the surface membrane of TRAIL-resistant cells (9). Many prostate cancer cell lines including ALVA-31, Du-145 and PC-3 are extremely sensitive to TRAIL and undergo apoptosis when exposed; however, other cell lines such as LNCaP are highly resistant (11). This resistance has been shown to be reversed by infection of those cells with Ad (12), treatment of the cells with radiation therapy (13), or simultaneous administration of chemotherapeutic agents such as paclitaxel, vincristine, vinblastine, etoposide, doxorubicin or camptothecin (14). For these reasons, TRAIL is a promising cytotoxic gene product for the molecular therapy of prostate cancer.

In this study, membrane-bound TRAIL cDNA was introduced into a prostate-specific replication-competent adenovirus (PSRCA), called Ad-IU-2, under the control of the chimeric prostate-specific enhancing sequence (PSES) which is comprised of the minimal sequences from prostate-specific antigen (PSA) androgen-responsive element core (AREc) and prostate-specific membrane antigen (PSMA) enhancer (PSME) which retained the highest prostate-specific activity. PSES was found to be active in PSA/PSMA-positive cells and demonstrated five-fold higher activity than universal promoter RSV and activity equal to CMV promoter (15).

Furthermore, adenoviral *E1a* and *E4* genes were placed under the control of PSES upstream from the right ITR as well as *E1b* in addition to TRAIL cDNA under the control of PSES downstream of the left ITR.

The antitumor activity of Ad-IU-2 was investigated both *in vitro* in PSA/PSMA-positive androgen-independent cell lines and *in vivo* in androgen-independent CWR22rv nude mice xenografts. The killing activity of Ad-IU-2 was observed to be two-fold greater than that of compared to a PSRCA with a similar backbone as Ad-IU-2. This augmentation of killing power was due to TRAIL-mediated cytotoxicity. Ad-IU-2 inhibited the growth of subcutaneous CWR22rv xenografts, and is expected to demonstrate strong clinical activity against heterogenous prostate tumors due to its TRAIL-mediated bystander killing effect.

Materials and Methods

Cell culture.

The packaging cell line HER911E4 stably expresses the adenoviral *E4* gene under control of the inducible *tetR* promoter (16) and was derived from the human embryonic retinoblast (HER911) cell line which was transformed with a plasmid containing the adenoviral genome (bp 79-5789) (17). HER911E4 cells were cultured in DMEM supplemented with 10% fetal bovine serum (FBS) (Atlanta Biologicals, Lawrenceville, GA), 1% penicillin-streptomycin (Gibco, Grand Island, NY), 0.1 mg/ml hygromycin B (Calbiochem, San Diego, CA) and 2 μg/ml doxycycline (Sigma, St. Louis, MO). CWR22rv is an androgen-independent, PSA/PSMA-positive prostate cancer cell line derived by the propagation of the androgen-dependent parental xenograft, CWR22, in nude mice (18). LNCaP is an androgen-dependent, PSA/PSMA-positive prostate cancer cell line established from a lymph node of a patient with metastatic disease (19). C4-2, an androgen-independent, PSA/PSMA-positive prostate cancer line, was derived by co-injection of LNCaP and bone stromal cells into nude mice (20). PC-3 is an androgen-independent prostate cancer cell that is slightly PSA-positive and PSMA-negative, and it was originally derived from the bone marrow aspirates of a patient with bone metastases (21). DU-145, an androgen-independent prostate cancer cell, is PSA/PSMA-negative and was derived from a brain lesion in a patient with confirmed metastatic disease (22). All prostate cancer cell lines were cultured in RPMI 1640 supplemented with 10% FBS and 1% penicillin-streptomycin. Adult human dermal fibroblasts (HDFa) were cultured in Medium 106 supplemented with 2% FBS, 1 μg/ml hydrocortisone, 10 ng/ml human epidermal growth factor, 3 ng/ml basic fibroblast growth factor and 10 μg/ml heparin (Cascade Biologics, Portland, OR). All cells were maintained at 37^{o}C and 5% CO_2.

Adenoviral vectors.

Ad-IU2 was developed by modifying Ad-E4PSESE1a, the previously described PSRCA with a cytomegalovirus (CMV) promoter-driven enhanced green fluorescent protein (EGFP) marker (23). To construct Ad-IU2, the human full-length *TRAIL* gene from pORF-hTRAIL (InvivoGen, San Diego, CA) was cloned downstream of PSES into pAd1020SfidA (OD 260, Boise, ID), the adenoviral cloning vector containing the left ITR and packaging signal, to make pAd1020SfidA-PSESTRAIL, which was further digested with *SfiI* to release the left ITR and PSES-TRAIL expression cassette. This fragment was cloned into pAd288E1b-E4PSESE1a (23), the modified adenoviral genome vector, and the ligation product was transformed into TOP10 *E. coli* competent cells (Invitrogen, Carlsbad, CA). The adenoviral genome (Fig. 1A) was released by digestion with *PacI* and transfected into HER911E4 cells with Lipofectamine 2000 (Invitrogen). Ad-IU2 was further amplified in HER911E4 cells and purified by CsCl centrifugation gradient and dialyzed, as described previously (23).

Replication-competent control viruses used in this study include Ad-E4PSESE1a and Ad-IU1. Ad-IU1 was constructed in a similar fashion as Ad-IU2; however, a PSES-HSV-TK expression cassette replaces the PSES-TRAIL expression cassette. Without administration of a nucleoside analog prodrug, the only cytotoxicity provided by Ad-IU1 is due to replication. Ad-E4PSESE1a was used as a negative control for all experiments except for FACS analysis, where EGFP would interfere with the Annexin V-FITC staining, and *in vivo,* where

To achieve equal bioactivity of Ad-IU2 and control viruses, a titer assay was performed

Western blot analysis.

For TRAIL expression, 1 x 10^6 CWR22rv cells were cultured overnight and infected with Ad-IU2 at an MOI of 1000 vp. As a positive control, CWR22rv cells were transfected with pORF-hTRAIL using Lipofectamine 2000. Media were changed 24 hours or 3 hours after infection or transfection, respectively. 48 hours after infection, cells were washed with cold PBS and harvested with radioimmunoprecipitation assay (RIPA) buffer containing 1 ml modified RIPA buffer, 20 μl 57 mmol/L phenylmethylsulfonyl fluoride and 2.5 μl phosphatase inhibitor cocktail (Sigma-Aldrich, St. Louis, MO). Cell lysates were kept on ice for 1 hour, centrifuged to pellet debris, and supernatants kept at -70^{o}C. Protein concentration was analyzed by Bradford assay (Bio-Rad, Hercules, CA), and 20 μg of protein (with or without 1M DTT) were separated by 4-10% SDS-PAGE and transferred to a nitrocellulose membrane. Membranes were blocked overnight at 4^{o}C in 5% fat-free milk and TBST and incubated with the primary antibodies

Results

TRAIL is expressed in a PSA/PSMA-dependent fashion.

The structure of Ad-IU-2 (Fig. 1A) is based on the PSRCA, Ad-E4PSESE1a, in which the *E1* promoter was deleted and *E1a* moved to the right ITR *E4* region under control of the bidirectional PSES enhancer sequence (23). Full-length, membrane-bound TRAIL cDNA was inserted at the left ITR in the *E1a* region upstream from adenoviral *E1b*, both under the control of PSES. As depicted in Figure 1B, full-length TRAIL protein expression was confirmed by western blot in PSA/PSMA-positive CWR22rv cells.

A 32 kD band was observed in the Western of cell lysates from cells infected by Ad-IU-2 (lanes 1, 3 and 5) but not by Ad-IU-3 (lanes 2, 4 and 6). Because TRAIL could be produced in cells, but not delivered to the membrane of the cell, TRAIL surface expression was detected by FACS analysis (Data not shown).

Ad-IU-2 was effective in inducing apoptosis in PSA/PSMA-positive cells.

PSA/PSMA-positive prostate cancer cells, CWR22rv, C4-2 and LNCaP, as well as PSA/PSMA-negative cell lines, PC-3, DU-145 and HeLa, were seeded in a 12-well plate, and infected with 1000 vp Ad-IU-1, Ad-IU-2 or no virus 24 hours after plating. Cells were analyzed 24 hours after infection by FACS using AnnexV and PI (Fig. 2). Following Ad-IU-1 infection, no significant apoptosis was induced above baseline levels. Ad-IU-1, which replaces TRAIL cDNA with HSV-TK, was used to determine the effect of viral replication on apoptosis induction, as without the addition of a nucleoside analogue, such as ganciclovir, in the media, Ad-IU-1 kills prostate cancer cells merely by viral replication. As host cell lysis and apoptosis occurs late in

adenoviral infection, no significant apoptosis was expected in the Ad-IU-1 infected group. Apoptosis following Ad-IU-2 infection was induced 5-fold higher in PSA/PSMA-positive CWR22rv and C4-2 cells above baseline apoptosis. As expected, no apoptosis above baseline level was in PC-3, DU-145 and HeLa cells. LNCaP, a PSA/PSMA-positive prostate cancer cell line that expresses Ad-IU-2 delivered TRAIL (Fig. 1C) did not apoptose following Ad-IU-2 infection (Fig. 2). This was expected, as LNCaP cells are highly resistant to the cytotoxic effects of TRAIL (24).

Ad-IU-2 effectively killed prostate cancer cells, while it spared normal cells.

To assure that apoptosis induction and viral replication within cells was sufficient to kill prostate cancer cells, an *in vitro* killing assay was performed. Infection of CWR22rv cells at serial dilutions ranging from 0 to 1 x 10^1 IFU/Cell of wild-type adenovirus, Ad-IU-1, Ad-IU-2 and replication-deficient Ad-PSES-Luc (negative control) was performed 24 hours following the seeding of 1.5 x 10^5 cells/well. As illustrated in Figure 3A, attached cells were stained with crystal violet. Ad-IU-2 effectively cleared all cells at a concentration of 1 IFU/Cell, whereas, Ad-IU-1 required a higher dose of 10 IFU/Cell to clear the well. Ad-Wt cleared wells at the lowest concentration, 0.1 IFU/Cell. Therefore, the killing power of Ad-IU-2 was 10-fold greater than that of Ad-IU-1 and 10-fold weaker than that of Ad-Wt. The negative control Ad-PSES-Luc virus demonstrated toxicity at the highest concentration. This was thought to be due to late adenoviral expression of *E3* transcripts from the *Major Late Promoter*. The similar experiment was repeated using normal human fibroblasts. As illustrated in Figure 3B, neither Ad-IU-1 nor Ad-IU-2 killed human fibroblasts. On the other hand, Ad-Wt demonstrated cytotoxicity at even

the lowest infectious concentration tested. Similar as in CWR22rv cells, the highest dose of Ad-PSES-Luc resulted in complete clearing of the cells.

Ad-IU-2 inhibited the growth of subcutaneous, androgen-independent CWR22rv xenografts.

Subcutaneous CWR22rv tumors were induced by injecting 2 x 10^6 CWR22rv cells into the bilateral flanks of castrated, athymic mice. After 3 weeks, when palpable tumors were stable, intratumoral injections of Ad-IU-2, Ad-E1aPSESE4 (genomic backbone of Ad-IU-2) or PBS were administered. As depicted in Figure 4A, untreated tumor volume and separated from virally-treated tumors after 1 week. Untreated mice were sacrificed at 5 weeks due to overwhelming tumor burden. Ad-IU-2 suppressed the growth of subcutaneous CWR22rv xenografts significantly than Ad-E1aPSESE4, especially at 5 and 6 weeks (15-fold growth, compared to 3-fold growth in tumor volume). Of the 7 tumors treated with Ad-IU-2, 6 responded favorably to treatment. Two tumors were completely eradicated 3 weeks post-treatment, and 4 tumors reduced in tumor volume to 0.4-fold of the original tumor volume (Fig. 4B). Tumors were followed for 6 weeks, at which time they were sectioned and stained with hematoxylin and eosin. As depicted in Figure 4C, PBS-treated CWR22rv tumors contained cells that appeared healthy and assumed normal CWR22rv xenograft architecture. Significant tumor vasculature was observed in the margins of the growing tumor. Necrosis was only detected in the center of the tumor, and is attributed to the hypoxic environment within the center of large tumors. Ad-IU-2 treated tumors (Fig. 4D) displayed diffuse necrosis and disruption of the normal tumor architecture in the margins of the tumor. The edematous nature of the treated tumors reflects damage to the tumors. Gross tumor vasculature was significantly reduced in the

Ad-IU-2 treated tumors. As depicted in Figure 4 E, treatment with Ad-IU-2 resulted in apoptosis induction in nuclei scattered and surrounding necrotic centers of viral injection.

Ad-IU-2 killing can be augmented by a TRAIL-mediated bystander effect.

Because human prostate tumors are heterogeneous cancers with varied expression profiles, foci of PSA/PSMA-negative cancer cells could co-exist with PSA/PSMA-positive cells. Without the ability to target the PSA/PSMA-negative prostate cancer cells, the entire tumor mass cannot be eliminated. PSA/PSMA-negative PC-3 cells were stably transfected with pCDNA3.1-mRFP-hrl to label all non-receptive cells. These cells were co-cultured with Ad-IU-1 or Ad-IU-2 infected CWR22rv cells after washing the cells to remove excess virus. As depicted in Figure 5A, labeled PC-3 cells, once resistant to the current treatment (Fig. 2), were caused to induce significant levels of apoptosis above that of baseline or Ad-IU-1 treated cells. TRAIL expression on the surface of Ad-IU-2 infected CWR22rv cells contacting PC-3 cells induced apoptosis in the mRFP-labeled cells. This was evidenced by the fact that increasing plating concentrations of CWR22rv cells resulted in greater apoptosis induction in PC-3 cells.

To show that the TRAIL-mediated bystander effect also resulted in the late event of cell death, relative cell counts of stably transfected CWR22rv-luc and PC-3-mRFP-hrl were determined one week after infection of receptive cells and co-culture with non-receptive cells. Firefly luciferase and renilla luciferase activities were found to correlate well with CWR22rv-luc and PC-3-mRFP-hrl cell counts, respectively (data not shown). As illustrated in Figure 5B, as expected, infection with Ad-IU-1 and Ad-IU-2 resulted in reduction of relative luciferase activity, correlating with a decrease in CWR22rv cell number. As illustrated in Figure 5C, all ratios receptive-to-non-receptive cells resulted in an increase in the number of PC-3-mRFP-hrl cells, as

compared to the untreated co-cultures; however, treatment with Ad-IU-2 resulted in similar or reduced renilla activity as the untreated cells. As treatment with both Ad-IU-1 and Ad-IU-2 resulted in reduction of CWR22rv cells, co-cultured PC-3 cells in those infected wells could grow as space once occupied by CWR22rv cells was freed. Through the TRAIL-mediated bystander effect, Ad-IU-2 effectively killed PC-3 cells, whereas Ad-IU-1 was not able to kill PC-3 cells, resulting in a spike in relative renilla activity.

Discussion

As dose-limiting toxicities and resistance to failures threaten the successful clinical treatment of hormone-refractory prostate cancer, novel therapies must be investigated. Recently, our laboratory has demonstrated the promising potential of gene therapy for advanced prostate in early clinical trials (25). Limitations of current trials and applications include the low viral transduction of replication-deficient adenoviral vectors. Ad-IU-2 has demonstrated tight control of replication and transgene expression in PSA/PSMA-positive prostate cancer cells. Systemic delivery of the virus would result in the capability to target distant metastases or locally recurrent tumors without causing damage to adenoviral tropic tissues such as liver or respiratory epithelium. Furthermore, as the prostate is a non-essential organ post-fertility, complete eradication of the prostate epithelium could serve as a cancer therapeutic or cancer preventative measure.

Ad-IU-2 effectively induced apoptosis in receptive, PSA/PSMA-positive cells, and this was correlated to strong *in vitro* killing ability. The addition of TRAIL to a PSRCA augmented the killing power of a replication-competent virus. Limitations of the current therapy include the ineffectiveness of this virus to induce apoptosis in TRAIL-resistant cells such as LNCaP. Mechanisms of resistance include Akt overexpression and TRAIL receptor downregulation. Fortunately, treatment of resistant cells with DNA-damaging agents has been shown to upregulate the expression of TRAIL receptors, DR-4 and DR-5 (14, 24).

Ad-IU-2 demonstrated promising success in reducing tumor volume and inhibiting growth of subcutaneous CWR22rv castrated athymic mouse xenografts. One limitation of

several adenoviral vectors currently in preclinical studies is a rebound in tumor size after 3 to 4 weeks of treatment. This is thought to be caused by inactivation of the virus in a hypoxic environment or induction of angiogenesis, allowing the tumor growth to overcome adenoviral replication. As observed in Ad-IU-2 treated tumors, TRAIL may inhibit the growth of tumor-specific neovasculature, thereby further inhibiting tumor growth.

Important to the clinical success of a PSA/PSMA-restricted replication-competent adenovirus is the ability to target PSA/PSMA-negative cells also present in heterogeneous prostate tumors. Ad-IU-2 infection resulted in a bystander killing effect that was TRAIL-mediated. This bystander effect could be further improved by expressing soluble forms of TRAIL that are secreted in the tumor matrix. In combination with chemotherapy, a PSRCA armed with a cytotoxic molecule able to induce bystander killing, will show great promise in the treatment of advanced androgen-independent prostate cancer.

References

1. Jemal A, Siegel R, Ward E*, et al.* Cancer statistics, 2006. CA Cancer J Clin 2006;56: 106-30.
2. Coen JJ, Zietman AL, Thakral H, Shipley WU. Radical radiation for localized prostate cancer: local persistence of disease results in a late wave of metastases. J Clin Oncol 2002;20: 3199-205.
3. Han M, Partin AW, Pound CR, Epstein JI, Walsh PC. Long-term biochemical disease-free and cancer-specific survival following anatomic radical retropubic prostatectomy. The 15-year Johns Hopkins experience. Urol Clin North Am 2001;28: 555-65.
4. Chodak GW, Keane T, Klotz L. Critical evaluation of hormonal therapy for carcinoma of the prostate. Urology 2002;60: 201-8.
5. Petrylak DP, Tangen CM, Hussain MH*, et al.* Docetaxel and estramustine compared with mitoxantrone and prednisone for advanced refractory prostate cancer. N Engl J Med 2004;351: 1513-20.
6. Tannock IF, de Wit R, Berry WR*, et al.* Docetaxel plus prednisone or mitoxantrone plus prednisone for advanced prostate cancer. N Engl J Med 2004;351: 1502-12.
7. Wiley SR, Schooley K, Smolak PJ*, et al.* Identification and characterization of a new member of the TNF family that induces apoptosis. Immunity 1995;3: 673-82.
8. Pitti RM, Marsters SA, Ruppert S, Donahue CJ, Moore A, Ashkenazi A. Induction of apoptosis by Apo-2 ligand, a new member of the tumor necrosis factor cytokine family. J Biol Chem 1996;271: 12687-90.
9. Pan G, Ni J, Wei YF, Yu G, Gentz R, Dixit VM. An antagonist decoy receptor and a death domain-containing receptor for TRAIL. Science 1997;277: 815-8.
10. Pan G, O'Rourke K, Chinnaiyan AM*, et al.* The receptor for the cytotoxic ligand TRAIL. Science 1997;276: 111-3.
11. Nesterov A, Lu X, Johnson M, Miller GJ, Ivashchenko Y, Kraft AS. Elevated AKT activity protects the prostate cancer cell line LNCaP from TRAIL-induced apoptosis. J Biol Chem 2001;276: 10767-74.
12. Voelkel-Johnson C, King DL, Norris JS. Resistance of prostate cancer cells to soluble TNF-related apoptosis-inducing ligand (TRAIL/Apo2L) can be overcome by doxorubicin or adenoviral delivery of full-length TRAIL. Cancer Gene Ther 2002;9: 164-72.
13. Shankar S, Singh TR, Srivastava RK. Ionizing radiation enhances the therapeutic potential of TRAIL in prostate cancer in vitro and in vivo: Intracellular mechanisms. Prostate 2004;61: 35-49.
14. Shankar S, Chen X, Srivastava RK. Effects of sequential treatments with chemotherapeutic drugs followed by TRAIL on prostate cancer in vitro and in vivo. Prostate 2005;62: 165-86.
15. Lee SJ, Kim HS, Yu R*, et al.* Novel prostate-specific promoter derived from PSA and PSMA enhancers. Mol Ther 2002;6: 415-21.
16. He TC, Zhou S, da Costa LT, Yu J, Kinzler KW, Vogelstein B. A simplified system for generating recombinant adenoviruses. Proc Natl Acad Sci U S A 1998;95: 2509-14.
17. Fallaux FJ, Kranenburg O, Cramer SJ*, et al.* Characterization of 911: a new helper cell line for the titration and propagation of early region 1-deleted adenoviral vectors. Hum Gene Ther 1996;7: 215-22.

18. Sramkoski RM, Pretlow TG, 2nd, Giaconia JM*, et al.* A new human prostate carcinoma cell line, 22Rv1. In Vitro Cell Dev Biol Anim 1999;35: 403-9.
19. Horoszewicz JS, Leong SS, Kawinski E*, et al.* LNCaP model of human prostatic carcinoma. Cancer Res 1983;43: 1809-18.
20. Wu HC, Hsieh JT, Gleave ME, Brown NM, Pathak S, Chung LW. Derivation of androgen-independent human LNCaP prostatic cancer cell sublines: role of bone stromal cells. Int J Cancer 1994;57: 406-12.
21. Kaighn ME, Narayan KS, Ohnuki Y, Lechner JF, Jones LW. Establishment and characterization of a human prostatic carcinoma cell line (PC-3). Invest Urol 1979;17: 16-23.
22. Stone KR, Mickey DD, Wunderli H, Mickey GH, Paulson DF. Isolation of a human prostate carcinoma cell line (DU 145). Int J Cancer 1978;21: 274-81.
23. Li X, Zhang YP, Kim HS*, et al.* Gene therapy for prostate cancer by controlling adenovirus E1a and E4 gene expression with PSES enhancer. Cancer Res 2005;65: 1941-51.
24. Munshi A, McDonnell TJ, Meyn RE. Chemotherapeutic agents enhance TRAIL-induced apoptosis in prostate cancer cells. Cancer Chemother Pharmacol 2002;50: 46-52.
25. Kubo H, Gardner TA, Wada Y*, et al.* Phase I dose escalation clinical trial of adenovirus vector carrying osteocalcin promoter-driven herpes simplex virus thymidine kinase in localized and metastatic hormone-refractory prostate cancer. Hum Gene Ther 2003;14: 227-41.

Figure Legends

Figure 1. Genomic structure and targeted expression of Ad-IU-2. A, TRAIL cDNA is placed at the left ITR under control of the bidirectional PSES enhancer. To avoid interference with the adenoviral packaging signal (ψ), *E1a* was placed at the right ITR under the transcriptional control of PSES along with *E4*. B, Adenoviral E1a proteins were detected by Western blot from 36 kD to 50 kD. E1a expression was limited to PSA/PSMA-positive prostate cancer cell lines after Ad-IU-2 infection. PSA/PSMA-positive prostate cancer cell lines, C4-2, CWR22rv and LNCaP and PSA/PSMA-negative prostate cancer cells, DU145 and PC-3 were infected with 100 vp/cell Ad-IU-1 (expressing HSV-TK in place of TRAIL), Ad-IU-2 or wild-type adenovirus. Cell lysates were probed with β-actin as a loading control. C, TRAIL was expressed in PSA/PSMA-positive cells. C4-2, LNCaP and CWR22rv cells were infected with 100 vp Ad-IU-2 or Ad-IU-3 (expressing FasL) as a negative control. Cell lysates were analyzed by Western blot 48 hours after infection. A 32 kD band was observed in lanes 1,3 and 5 but not in cells infected with Ad-IU-3 (lanes 2, 4 and 6).

Figure 2. Ad-IU-2 induced apoptosis in PSA/PSMA-positive prostate cancer cells. Cells were infected with 100 vp Ad-IU-1 (prostate-specific replication-competent adenovirus) or Ad-IU-2. Cells were analyzed 24 hours after infection by FACS analysis with AnnexinV/PI staining. Untreated levels represented basal levels of apoptosis for each cell line, and levels induced by Ad-IU-1 represented apoptosis induced by replication of the virus. Apoptosis was markedly induced in CWR22rv and C4-2 cells, n = 5 each group, * = $p<0.05$.

Figure 3. Ad-IU-2 killed PSA/PSMA-positive cells *in vitro*, but spared normal human fibroblasts. 1.5 x 10^5 CWR22rv cells or human fibroblasts were plated and infected with wild-type adenovirus, replication-defective Ad-PSES-Luc, Ad-IU-2 or Ad-IU-1 at serial dilutions 24 hours after plating. Plates were stained with crystal violet 7 days after infection. Cleared wells indicated complete viral killing.

Figure 4. *In vivo* evaluation of Ad-IU-2. A, Subcutaneous androgen-independent prostate tumors were induced by injecting 2 x 10^6 CWR22rv cells per site on bilateral flanks of castrated male nude mice. 3 weeks after the appearance of palpable tumors, 2 x 10^7 IFU of Ad-IU-2 or E1aPSESE4 (a prostate-specific replication-competent adenovirus with similar backbone as Ad-IU-2) was injected intratumorally. Ad-IU-2 suppressed the growth CWR22rv tumors 6-fold better than E1aPSESE4, suggesting that TRAIL enhanced the *in vivo* killing power of an oncolytic virus. B, six of seven tumors responded to treatment by Ad-IU-2. Four tumors decreased in volume after treatment with Ad-IU-2, and 2 tumors were completely eradicated 3 weeks post-treatment. The non-responder experienced 15-fold growth in volume by week 5 of treatment. Tumors were harvested at 6 weeks, fixed, embedded in paraffin and stained with haematoxylin and eosin. Images are representative of tumors in either untreated (C) or Ad-IU-2 treated (D) groups. All images were taken at 40X. C, Untreated tumors appeared healthy with little necrosis in the growing tumor margin. Significant vascularization was observed the untreated tumors, indicative of a rapidly growing tumor. D, Cells in the Ad-IU-2 treated tumors appeared unhealthy. Wide-spread necrosis, edema and infrequent vasculature were observed throughout the majority of the tumors. E, *In vivo* TUNEL assay of Ad-IU-2 treated tumor revealed widespread apoptosis around the necrotic center of the tumor.

Figure 5. *In vitro* demonstration of a TRAIL-mediated bystander effect. A, PSA/PSMA positive CWR22rv cells were plated in a 12-well plate and infected with 100 vp Ad-IU-1 or Ad-IU-2 24 hours later. Twenty-four hours after infection, the wells were washed with 3X with 1X PBS. Following the washing, mRFP-hrl stably transfected PSA/PSMA-negative PC-3 cells were co-plated in the indicated ratios. Percent apoptotic PC-3 cells was measured by FACS analysis. Ad-IU-2 significantly induced apoptosis in PC-3 cells as compared to basal level and Ad-IU-1 treated cells, $p = <0.05$. Human firefly luciferase stably transfected CWR22rv were plated in a 12-well plate and infected with 100 vp Ad-IU-1 or Ad-IU-2 24 hours later. Twenty-four hours after infection, the wells were washed with 3X with 1X PBS. Following the washing, mRFP-hrl stably transfected PC-3 cells were co-plated in the indicated ratios. B, Cells were lysed and luciferase assay was performed after 7 days in co-culture. A decrease in luciferase activity represented a decrease in CWR22rv cell count as compared to the untreated group. C, A decrease in renilla activity represented a decrease in PC-3 cell count, $n = 4$ each group, * = $p<0.05$.

Combination therapy of androgen-independent prostate cancer using a prostate restricted replicative adenovirus and a replication-defective adenovirus encoding human endostatin-angiostatin fusion gene

Xiong Li,[1,5] Sudhanshu P. Raikwar,[1,5] You-Hong Liu,[1,5] Sang-Jin Lee,[1,5] Yan-Ping Zhang,[1,5] Shaobo Zhang,[4] Liang Cheng,[1,4] Sang-Don Lee,[1,5] Beth Elisa Juliar,[6] Thomas A. Gardner,[1,2,5] Meei-Huey Jeng,[2,3,5] and Chinghai Kao[1,2,5]

Departments of [1]Urology, [2]Microbiology and Immunology, [3]Medicine, and [4]Pathology, [5]Walther Oncology Center, and [6]Division of Biostatistics, Indiana University School of Medicine, Indianapolis, Indiana

Abstract

Although prostate-restricted replicative adenovirus has exhibited significant antitumor efficacy in preclinical studies, it is necessary to develop more potent adenoviruses for prostate cancer gene therapy. We evaluated the synergistic killing effect of prostate-restricted replicative adenovirus and AdEndoAngio, a replication-defective adenovirus expressing the endostatin-angiostatin fusion protein (EndoAngio). When coadministered with AdEndoAngio, prostate-restricted replicative adenovirus significantly elevated EndoAngio expression, suggesting that AdEndoAngio coreplicates with prostate-restricted replicative adenovirus. Conditioned medium from prostate cancer cells infected by prostate-restricted replicative adenovirus plus AdEndoAngio inhibited the growth, tubular network formation, and migration of human umbilical vein endothelial cells better than conditioned medium from prostate cancer cells infected by AdEndoAngio alone. Furthermore, *in vivo* animal studies showed that the coadministration of prostate-restricted replicative adenovirus plus AdEndoAngio resulted in the complete regression of seven out of eight treated androgen-independent CWR22rv tumors, with a tumor nodule maintaining a small size for 14 weeks. The residual single tumor exhibited extreme pathologic features together with more endostatin-reactive antibody-labeled tumor cells and fewer CD31-reactive antibody-labeled capillaries than the AdEndoAngio-treated tumors. These results show that combination therapy using prostate-restricted replicative adenovirus together with antiangiogenic therapy has more potent antitumor effects and advantages than single prostate-restricted replicative adenovirus and deserves more extensive investigation. [Mol Cancer Ther 2006; 5(3):676–84]

Introduction

Prostate cancer is the second leading cause of male cancer-related deaths in the U.S. In 2005, it is estimated that new diagnoses of this disease may be second only to skin cancer, affecting 232,090 men, and that roughly 30,350 men will die from this disease in the U.S. Whereas early detection and several therapeutic approaches for locally confined prostate cancer offer excellent chances for long-term cure, 20% to 25% of patients will experience local recurrence and progress to advanced stage disease. Currently, the only treatment modality available for patients with advanced disease is hormone ablation therapy because prostate cancer proliferation is critically dependent on androgen. However, tumor regression is temporary and the disease inevitably progresses to androgen independent status.

Gene therapy offers a unique opportunity for androgen-independent prostate cancer treatment. A number of limitations, however, lead to the suboptimal efficacy of existing gene therapies. Over the past 10 years, gene therapy has not shown significant clinical success. These limitations include (*a*) low gene transfer efficiency by therapeutic vectors, (*b*) weak potency of therapeutic genes, (*c*) inadequate bystander effect, and (*d*) the molecular heterogeneity of prostate tumors (1). Because ONYX-015 virus has shown promise for cancer gene therapy, tumor/tissue-restricted replicative adenoviruses have drawn a lot of attention. The initial viral infection of the target cell can produce progeny virions that infect adjacent cancer cells, thereby improving *in vivo* infectivity, biodistribution, and bystander effects mediated by adenovirus (2, 3). However, tumor/tissue-restricted replicative adenoviruses exhibited only limited therapeutic efficacy in clinical trials when used as a monotherapy (4–6). To improve the efficacy of tumor/tissue-restricted replicative adenoviruses, they need to be combined with other therapeutic agents.

Angiogenesis is controlled by a balance between angiogenic stimulators and inhibitors. This balance is perturbed in tumors by either overproduction of angiogenic inducers

Received 8/26/05; revised 1/3/06; accepted 1/18/06.

Grant support: NIH grant CA074042 (C. Kao), DOD grant W23RX-3270-N729 (C. Kao).

The costs of publication of this article were defrayed in part by the payment of page charges. This article must therefore be hereby marked advertisement in accordance with 18 U.S.C. Section 1734 solely to indicate this fact.

Requests for reprints: Chinghai Kao, Department of Urology, Indiana University School of Medicine. 1001 West 10th Street, Room OPW 320, Indianapolis, IN 46202. Phone: 317-278-6873; Fax: 317-278-3432. E-mail: chkao@iupui.edu

doi:10.1158/1535-7163.MCT-05-0339

or underproduction of angiogenic inhibitors (7). Among many angiogenesis regulators, endostatin, which is a carboxyl-terminal proteolytic fragment of collagen XVIII, is the most potent angiogenesis inhibitor. It blocks endothelial cell proliferation, migration/invasion, and tubular network formation. Therapeutically, endostatin inhibits tumor growth and angiogenesis in a wide variety of animal tumor models with little toxicity, immunogenicity, and resistance (8, 9). Angiostatin, an amino-terminal fragment of plasminogen, also shows potent antiangiogenic and/or antitumor effects. Recombinant adenoviral vectors encoding angiostatin cDNA have elicited high antitumor and antimetastatic effects (10, 11).

Recently, an endostatin and angiostatin fusion protein, EndoAngio, was developed and exhibited prolonged half-life and greater antiangiogenic effects (12). It has been reported that its replication-deficient therapeutic adenovirus can coamplify with tumor/tissue-restricted replicative adenoviruses (1, 13). The resulting selective production of large numbers of therapeutic adenovirus particles *in situ* within a tumor mass could transduce neighboring tumor cells and increase overall transduction efficiency (1). In this study, we used a prostate-restricted replication adenovirus combined with a replication-defective adenovirus encoding EndoAngio cDNA for optimal therapeutic effects in androgen-independent prostate cancers. We postulate that prostate-restricted replicative adenovirus will augment the transduction effect and expression of antiangiogenic factor protein locally, confining tumor growth. Additionally, tumor/tissue-restricted replicative adenoviruses can become more effective, causing complete regression of the tumor mass by killing existing tumor cells whereas their growth phase remains inhibited. In this report, we investigated the synergic antitumor effect of combinational therapy with prostate-restricted replicative adenovirus and this antiangiogenic modality.

Materials and Methods

Cells and Cell Culture

Human umbilical vein endothelial cells (HUVEC) were obtained from Cambrex Bio Science (East Rutherford, NJ) and were maintained in endothelial-specific medium EGM-2 (Cambrex) according to the manufacturer's instructions. Human embryonic retinoblast (HER911, a gift from Leiden University and Crucell, Leiden, the Netherlands) was cultured in DMEM supplemented with 10% fetal bovine serum (FBS) and 1% penicillin/streptomycin. HER911E4, which is a HER911 derivative with adenoviral *E4* gene under the control of *tetR* (14), was maintained in HER911 culture medium additionally supplemented with 0.1 mg/mL hygromycin B (Calbiochem, San Diego, CA) and 2 μg/mL doxycycline (Sigma, St. Louis, MO). HEK293 is a transformed human embryonic kidney cell line that expresses complementing adenoviral E1 proteins supporting the replication of *E1*-deleted recombinant adenoviruses. HEK293 was maintained in MEM (Invitrogen, Carlsbad, CA) containing 10% FBS, 1% penicillin/streptomycin, and 1% MEM nonessential amino acids. Prostate cancer cell lines C4-2, CWR22rv, PC-3, and DU145 were all maintained in RPMI 1640 supplemented with 10% FBS and 1% penicillin/streptomycin.

Construction of Recombinant Adenoviruses

The construction of the AdE4PSESE1a prostate-restricted replicative adenovirus was described in detail in an earlier publication (3). To construct a recombinant adenovirus (AdEndoAngio) expressing EndoAngio, the entire expression cassette including EF1α-human T-cell lymphotrophic virus promoter, human endostatin-angiostatin fusion gene, and polyadenylic acid signal was excised from pBlast-hEndo-angio expression vector (Invivogen, San Diego, CA) and subcloned into the adenoviral transfer vector pΔE1sp1A (Microbix Biosystems, Ontario, Canada), resulting in the plasmid pΔE1sp1A-hEndo-angio. These adenoviral transfer vectors were cotransfected with adenoviral vector pJM17 into HEK293 cells and generated the desired replication-defective recombinant adenovirus, AdEndoAngio.

Preparation of Conditioned Medium

CWR22rv cells (4×10^6) were plated in 100-mm culture dishes 24 hours before virus infection. The cells were infected by 100 virus particles (v.p.) per cell of AdE4PSESE1a or AdEndoAngio, or both 50 v.p. per cell of AdE4PSESE1a and 50 v.p. per cell of AdEndoAngio. The media were changed 8 hours post-viral infection. The conditioned medium was harvested 1 or 3 days after viral infection and concentrated by Centricon YM10 (Millipore, Billerica, MA). The conditioned media collected were used for testing EndoAngio expression by Western blotting, and the conditioned media collected at 3 days were used for evaluating antiangiogenic activity on HUVEC *in vitro* by growth assay, tubular formation, and cell migration assay.

Western Blotting

Proteins (20 μg) from conditioned medium were subjected to SDS-PAGE separation and transferred to a PDEF membrane (Millipore) using a NOVEX gel system (Invitrogen). The transferred membrane was probed with an anti-endostatin antibody (Abcam, Cambridge, MA), followed by a horseradish peroxidase–conjugated anti-rabbit IgG secondary antibody (Santa Cruz Biotechnology, Inc., Santa Cruz, CA). Antibodies on membrane were visualized by chemiluminescence (Pierce, Rockford, IL).

Cell Proliferation Assay

HUVEC were plated in 96-well plates (1×10^4 cells per well) and exposed to 10 μg/mL of conditioned medium. Eight wells were used for each virus. The growth media were changed every other day and HUVEC proliferation was assayed 7 days after administration of conditioned medium by 3-(4,5-dimethylthiazol-2-yl)-2,5-diphenyltetrazolium bromide assay. The data were expressed as the percentage of live cells versus mock-infected cells and SD of three independent experiments. Comparisons were made between each single treatment and the combination treatment using one-way ANOVA.

Tubular Network Formation Assay

Tubular network formation on Matrigel was assayed according to a modified protocol described in a previous publication (15). Briefly, HUVEC cells were labeled with a red-fluorescent lipid dye 1,1′-dioctadecyl-3,3,3′,3′-tetramethylindocarbocyanine perchlorate (DiI), according to the manufacturer's instructions (Invitrogen). Twenty-four–well plates were coated with 250 μL of Matrigel at 4°C and incubated at 37°C for 30 minutes. HUVECs (2.5×10^4) in 100 μL of EGM-2 medium were labeled by DiI and mixed with 10 μg/mL of conditioned medium harvested from virus-infected cells as described above. The mixtures of HUVECs and conditioned medium were dispensed in each well and incubated for 8 hours. The cells were photographed under a fluorescent phase-contrast microscope at ×40 magnification. The tubular network formation was quantified by averaging the number of connecting branches in 10 randomly chosen fields. A two-factor analysis of AdE4PSESE1a and AdEndoAngio was done to test interaction using the control group as the zero level of each treatment, AdEndoAngio and AdE4PSESE1a. Comparisons were made between each single treatment and the combination treatment using one-way ANOVA. In addition, two-way ANOVA was used to test the interaction between AdEndoAngio and AdE4PSESE1a.

HUVEC Cell Migration Assay

The HUVEC cell migration assay was done as described by Schleef and Birdwell (16). Briefly, a confluent monolayer of red HUVEC cells stained by DiI on 24-well plates was scratched using a sterile 200 μL plastic pipette tip. Displaced cells were removed with three washes of PBS, and fresh EGM-2 medium containing CWR22rv conditioned medium (10 μg/mL) or PBS was added. Cells and cell gaps were observed by fluorescent phase-contrast microscopy at 0, 12, and 24 hours after scratching. The position of the scratched edge was noted and the migrated distance was compared. We quantified the gap distances with the SPOT software 4.1 (Diagnostic Instruments, Inc., Sterling Heights, MI). One-way ANOVA was done to compare the difference between each single treatment and the combination treatment. In addition, two-way ANOVA was used to test the interaction between AdEndoAngio and AdE4PSESE1a.

Animal Experiments

CWR22rv tumor models were established by injecting 2×10^6 cells s.c. in the right flank of athymic nude mice (6-week-old males). Mice were castrated 3 days after cell injection. Mice were randomly grouped when tumor size reached ~30 mm^3 at around 2 to 3 weeks after cell injections (10 tumors in the AdCMVGFP-treated group, 15 tumors in the AdE4PSESE1a-treated group, 16 tumors in the AdEndoAngio-treated group, and 8 tumors in the combination therapy group) and received intratumoral injections of 2×10^9 v.p. of AdCMVGFP, AdE4PSESE1a, AdEndoAngio, or 1×10^9 v.p. of AdE4PSESE1a and 1×10^9 v.p. of AdEndoAngio in combination in 50 μL 1× PBS by using a syringe with a 27-gauge needle. Tumor appearance and tumor sizes were monitored once every week and the tumor volumes were calculated by using the formula (length × $width^2 \times 0.5236$; ref. 17). Mice were sacrificed when tumor size exceeded 500 mm^3. Statistical analysis was done by SAS Version 9 (SAS Institute Inc., Cary, NC). One-way ANOVA was used to compare the tumor growth ratios between the combination treatment group versus each treatment alone. A Kaplan-Meier survival analysis was used to compare the combination treatment versus each treatment alone with an event defined at the first week of nonrecurrent tumor disappearance and with tumor progression as censored. A log-rank test was used to analyze differences in time to disappearance between treatments. To confirm the log-rank result, logistic regression was done to compare tumor disappearance versus nonregression between treatments. The model fit was verified using the Hosmer-Lemeshow goodness-of-fit test.

Histology and Immunohistochemistry

Tumors were removed, immediately fixed in buffered formalin, processed, embedded in paraffin, and cut into histologic sections. Tumor sections were stained with H&E according to the standard protocol. For the EndoAngio detection, a polyclonal rabbit antibody reactive to endostatin (Abcam) was used at a 1:200 dilution. For microvessel density analysis, rat monoclonal antibodies reactive to mouse CD31 (BD Biosciences, San Diego, CA) were used at a 1:200 dilution. The slides were reacted with primary antibodies overnight in a humidified chamber at 4°C. After being rinsed once with PBS, a biotinylated polyclonal anti-rabbit or anti-rat second antibody (BioGenex, San Ramon, CA) was applied to slides at a dilution of 1:500 and incubated for 1 hour. After washing with PBS, slides were incubated with avidin-peroxidase complex (Vector Laboratories, Burlingame, CA) for 1 hour, washed once with PBS, stained with freshly prepared diaminobenzidine solution for 15 minutes and counterstained with hematoxylin. The stained capillaries were quantified by averaging the counting of capillaries in 10 randomly chosen fields. One-way ANOVA was done to compare the difference between each single treatment and the combination treatment.

Results

Prostate-Restricted Replicative Adenovirus and AdE4PSESE1a Enhanced the Transgene Expression of AdEndoAngio by Coinfection

There have been several reports that transgene expression by a replication-defective adenovirus could be enhanced by coinfection with a tumor/tissue-restricted replicative adenovirus, presumably by coamplification (1, 13). To determine whether the EndoAngio fusion protein expression delivered by AdEndoAngio could be enhanced by coinfection of a prostate-restricted replicative adenovirus, AdE4PSESE1a, we analyzed the EndoAngio fusion protein expression following the infection of CWR22rv cells with AdE4PSESE1a, AdEndoAngio, or AdEndoAngio/AdE4PSESE1a (both viruses at half-dose). As shown in Fig. 1, conditioned medium harvested from the CWR22rv cells infected with AdEndoAngio (CM-AdEndoAngio) contained more proteins than conditioned medium harvested from the CWR22rv cells infected with AdEndoAngio/AdE4PSESE1a

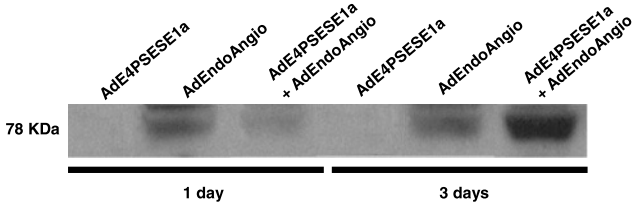

Figure 1. Elevated expression of EndoAngio fusion protein by cotransduction. CWR22rv cells were infected with AdE4PSESE1a, AdEndoAngio at 100 v.p. per cell, or the combination of 50 v.p. per cell of AdEndoAngio and 50 v.p. per cell of AdE4PSESE1a. The conditioned media were prepared as described in Materials and Methods. Then, 20 μg of proteins derived from the conditioned media from various virus-infected CWR22rv cells were subjected to Western blot analysis using an anti-endostatin antibody. The EndoAngio fusion protein-specific band was detected with an expected molecular weight of 78 kDa. AdE4PSESE1a significantly elevated the EndoAngio protein expression compared with the administration of AdEndoAngio alone.

(CM-AdEndoAngio/prostate-restricted replicative adenovirus) on day 1 after virus infection because we infected the cells with only a half-dose of AdEndoAngio in the combination group compared with AdEndoAngio alone. The expression of the fusion protein increased with time in CM-AdEndoAngio/prostate-restricted replicative adenovirus with more EndoAngio protein than in CM-AdEndoAngio alone on day 3. No fusion protein was detected in conditioned medium obtained from AdE4PSESE1a-infected cells (CM-prostate-restricted replicative adenovirus), as a negative control. These results suggest that coinfection with AdEndoAngio and AdE4PSESE1a could enhance the transgene expression of endostatin-angiostatin.

EndoAngio Inhibited the Biological Activities of HUVECs

To test whether the antiangiogenic activity of AdEndoAngio could be augmented by coinfection with AdE4PSESE1a, we did a HUVEC cell proliferation assay [3-(4,5-dimethylthiazol-2-yl)-2,5-diphenyltetrazolium bromide assay], cell migration assay, and tubular network formation assay (Matrigel assay) using the conditioned medium described above. Both CM-AdEndoAngio and CM-AdEndoAngio/prostate-restricted replicative adenovirus inhibited HUVEC proliferation (Fig. 2A). As expected from the amount of expressed fusion proteins in Fig. 1, CM-AdEndoAngio/prostate-restricted replicative adenovirus exerted much stronger growth-inhibitory effects on HUVECs compared with CM-AdEndoAngio ($P = 0.0002$) or CM-prostate-restricted replicative adenovirus ($P = 0.0005$) alone. In contrast, CM-prostate-restricted replicative adenovirus did not have any effect at all on the proliferation of HUVEC as well as conditioned medium harvested from PBS-treated CWR22rv cells (CM-PBS), implying that the inhibition of HUVEC proliferation was exclusively due to fusion proteins synthesized from the EndoAngio gene in AdEndoAngio adenovirus.

Assays of *in vitro* tubular network formation using HUVECs also confirmed that CM-AdEndoAngio/prostate-restricted replicative adenovirus elicited a stronger inhibitory effect on tubular network formation by HUVEC cells than CM-AdEndoAngio ($P < 0.0001$). The significant interaction between AdEndoAngio and AdE4PSESE1a in the two-way ANOVA analysis supports a synergistic effect between AdEndoAngio and AdE4PSESE1a ($P < 0.0001$). As expected, CM-prostate-restricted replicative adenovirus did not affect tubular network formation, compared with CM-PBS (Fig. 2B).

The migration ability of HUVECs was evaluated by an *in vitro* scratch wound assay. A confluent monolayer of HUVEC cells was artificially wounded by a 200 μL micropipette tip and incubated with conditioned medium harvested above. The migrating HUVEC cells could fill up the gaps 24 hours after incubation with CM-PBS and CM-prostate-restricted replicative adenovirus. In contrast, CM-AdEndoAngio markedly decreased HUVEC movement whereas CM-AdEndoAngio/prostate-restricted replicative adenovirus almost completely halted HUVEC movement at 24 hours after incubation. We quantified the gap distances with SPOT software 4.1. The CM-AdEndoAngio/prostate-restricted replicative adenovirus elicited a stronger inhibitory effect on the migration of HUVEC cells than CM-AdEndoAngio ($P < 0.0001$). The significant interaction between AdEndoAngio and AdE4PSESE1a in the two-way ANOVA analysis supports a synergistic effect between AdEndoAngio and AdE4PSESE1a ($P < 0.0001$; Fig. 2C). Collectively, these results clearly showed that coinfection had a stronger effect on HUVEC proliferation, migration and tubular network formation, and that AdE4PSESE1a and AdEndoAngio showed a synergistic effect.

Cotransduction Enhanced Antitumor Efficacy

We evaluated the antitumor efficacy of AdEndoAngio either alone or in combination with AdE4PSESE1a on the growth of androgen-independent CWR22rv s.c. tumors in athymic mice. As illustrated in Fig. 3A, the animal survival plot showed that only 20% of the mice survived in the AdE4PSESE1a intratumoral injection group and 37.5% of the mice survived in the AdEndoAngio group at 14 weeks. AdE4PSESE1a or AdEndoAngio alone inhibited tumor growth initially, compared with the AdCMVGFP-treated group, but most of the treated tumors eventually grew exponentially (Fig. 3B-D). On the other hand, coinjection of AdE4PSESE1a and AdEndoAngio resulted in complete regression of seven out of eight androgen-independent CWR22rv tumors in castrated nude mice hosts. One slow-growing nodule was kept to a small size for 14 weeks (Fig. 3E). Kaplan-Meier survival analysis was done using data through week 7 in order to include all tumor disappearance events and to minimize informative censoring (censoring related to tumor growth). Out of 23 total censored observations among the three treatment groups, 17 were censored at ≥7 weeks and 6 were censored due to animal sacrifice at weeks 5 or 6 (3 each). In statistical analysis, the combination of AdE4PSESEE1a and AdEndoAngio was superior to either AdE4PSESE1a or AdEndoAngio alone as tested by the log-rank test ($P = 0.0003$ and 0.046, respectively) and by logistic regression ($P = 0.008$ and 0.039, respectively). Goodness-of-fit of the logistic regression model was confirmed ($P > 0.999$). Median time to

disappearance in the combination treatment was 4 weeks (95% confidence intervals, 3–7 weeks). The results revealed enhanced therapeutic efficacy following oncolytic and antiangiogenic combination therapy in this androgen-independent prostate cancer animal model.

A Tumor Treated by Combinational Therapy Presents Distinct Pathologic Features

When a tumor from the intratumoral injection groups was harvested, we observed an interesting pathologic phenomenon in the single residual tumor mass treated by the combinational therapy. The tumor cells were arranged loosely in small patches surrounded by necrosis, and some of the tumor cells showed nuclei condensation and cytoplasmic acidophilia (the cytoplasm showed increased eosinophilia), suggesting that these tumor cells were undergoing necrosis (ref. 18; Fig. 4A). Randomly located patches and large foci of irregular necrosis were detected in AdE4PSESE1a-treated tumors, but the remaining tumor cells

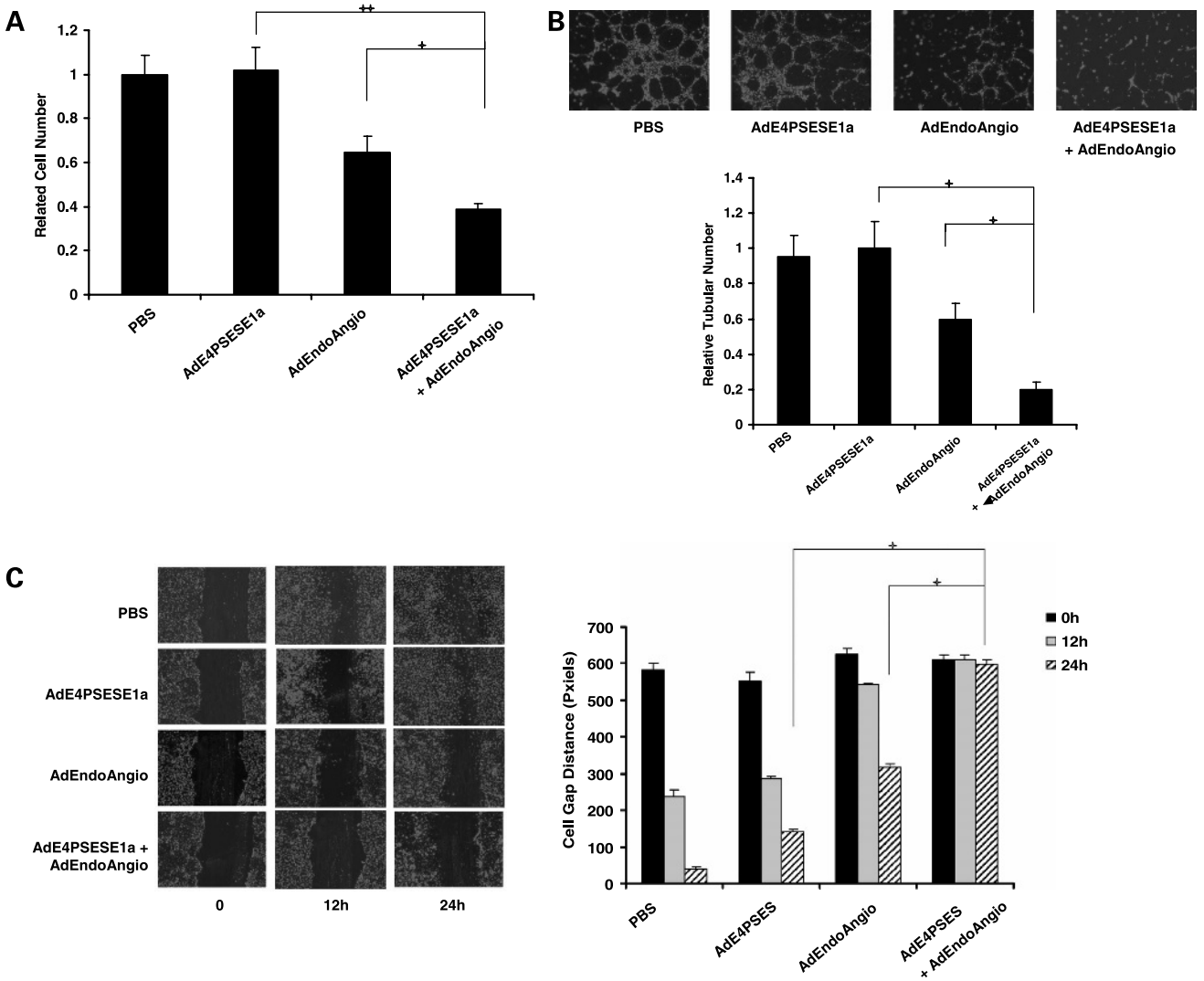

Figure 2. Biological activities of conditioned medium from virus-infected CWR22rv cells. **A,** conditioned medium from the combination therapy inhibits HUVEC proliferation. HUVEC cells (1×10^4/well) were seeded and subjected to 10 μg/mL of conditioned medium from AdE4PSESE1a-, AdEndoAngio-, combined virus-infected, or PBS-treated CWR22rv. Eight wells were used for each virus. 3-(4,5-Dimethylthiazol-2-yl)-2,5-diphenyltetrazolium bromide assay was done 7 d after conditioned medium treatment. *Columns,* the percentage of live cells versus mock-infected cells of three independent experiments; *bars,* SD; $^+$, $P = 0.0002$; $^{++}$, $P = 0.0005$. **B,** conditioned medium inhibits HUVEC tubular network formation. HUVEC cells (2.5×10^4) labeled by DiI were suspended in 100 μL EGM-2 medium and mixed with 10 μg/mL conditioned medium. The mixtures were dispensed in each well in 24-well plates coated with 250 μL Matrigel and incubated for 8 h. The cells were photographed and tubular network formation was quantified by counting the number of connecting branches between discrete endothelial cells. *Columns,* the percentage of live cells versus mock-infected cells of three independent experiments; *bars,* SD; $^+$, $P < 0.0001$. **C,** conditioned medium inhibits HUVEC migration. A confluent monolayer of red HUVEC cells labeled by DiI on 24-well plates was scratched using a sterile 200 μL plastic pipette tip. Displaced cells were removed with three washes, and fresh EGM-2 containing conditioned medium was added. The cell gaps were observed at 0, 12, and 24 h after scratching (see above). The cell gap was quantified by SPOT software and data are presented as above ($^+$ $P < 0.0001$). These results indicated that AdEndoAngio exerted a stronger antiangiogenic effect when coadministrated with a prostate-restricted replicative adenovirus *in vitro*.

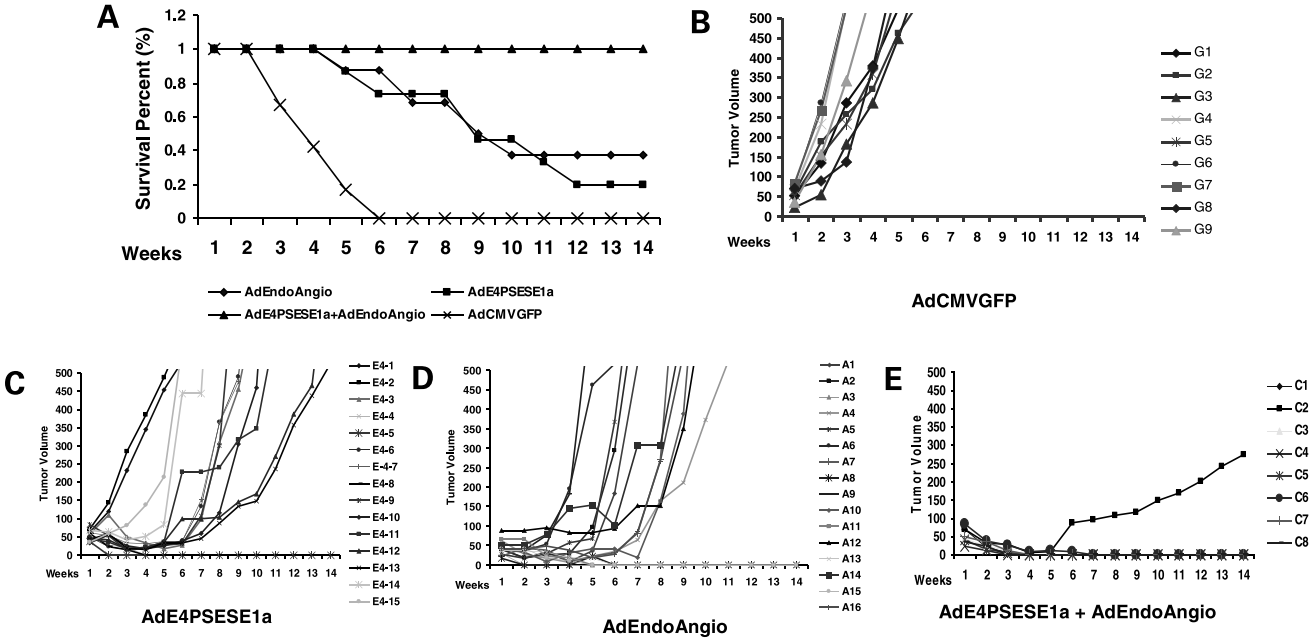

Figure 3. Evaluation of the antitumor effect of the combination modality *in vivo*. CWR22rv s.c. tumors were established in 6-wk-old athymic nude mice and treated with 2×10^9 v.p. of AdCMVGFP, 2×10^9 v.p. of AdE4PSESE1a, or 1×10^9 v.p. of AdE4PSESE1a plus 1×10^9 v.p. of AdEndoAngio. Tumor sizes were monitored once a week. Mice were sacrificed when tumor size exceeded 500 mm^3. **A,** Kaplan-Meier survival analysis; **B** to **E,** the tumor sizes of various adenovirus treatment groups. The results showed a superior therapeutic effect when combining AdEndoAngio with AdE4PSESE1a.

showed round/oval-shaped nuclei with fine granular chromatin, which indicated an active growing condition (Fig. 4B). The tumor cells in the AdEndoAngio-treated group showed no significant abnormal morphologic changes and no necrotic tissues could be detected inside the tumor mass (Fig. 4C). Again, the combination therapy showed a superior therapeutic effect to either AdE4PSESE1a or AdEndoAngio monotherapy. Immunohistochemical analysis revealed rich EndoAngio protein expression towards the periphery of the tumor mass in the cotransduction group (Fig. 4D), no EndoAngio protein expression in the AdE4PSESE1a-treated group (Fig. 4E), and only limited EndoAngio protein expression in the AdEndoAngio-treated group (Fig. 4F). Compared with the AdCMVGFP- (Fig. 5A), AdE4PSESE1a- (Fig. 5B), or AdEndoAngio-treated tumors (Fig. 5C), quantification of CD31 antibody-labeled capillaries revealed a significant decrease in capillary numbers within the residual tumor ($P < 0.0001$; Fig. 5D), although the labeled capillaries in the AdEndoAngio group also decreased significantly compared with AdCMVGFP-treated tumors ($P < 0.0001$). The labeled capillaries in the AdE4PSESE1a group showed a higher decrease compared with those in the AdEndoAngio group, mainly because of some big island-like necrotic areas inside the tumor masses.

Discussion

Our and other's previous investigations revealed that tumor/tissue-restricted replicative adenoviruses only partially suppress tumor growth in most solid tumors as a monotherapy. Limited viral spreading inside the tumor/tissue-restricted replicative adenovirus–treated tumor and healthy tumor growth away from loci of viral replication hamper tumor/tissue-restricted replicative adenovirus cell-killing efficacy (3). Therefore, targeting specific tumor cells may not be enough to generate an effective and durable response. Combinational gene therapy may achieve better clinical therapeutic efficacy by simultaneously attacking tumors at multiple levels and multiple targets.

The combination therapy includes adenoviruses armed with therapeutic genes (19–21), armed adenoviruses plus chemicals or cytokines (22) to improve the expression and efficiency of therapeutic genes, and coadministration of conditionally replication adenovirus and replication-defective adenovirus encoding the therapeutic genes (1). Several combination gene therapy modalities have reported improved effects compared with single modalities, by combining oncolytic adenovirus with pro-drug enzymes, apoptosis inducers (21), or angiogenesis inhibitors (19, 23, 24). The combination of replicative adenovirus and replication-defective adenovirus results in a far superior antitumor mechanism in which the cytotoxic effects are mediated by the replication-competent adenovirus, whereas therapeutic genes are simultaneously expressed in the local tumor microenvironment from the replication-defective adenoviral vector (1). In the present report, we coadministrated a prostate-restricted replicative adenovirus, AdE4PSESE1a, and a replication-defective adenovirus, AdEndoAngio, against androgen-independent prostate cancers. Consistent with other reports (1, 13), the combination therapy significantly improved the expression

of EndoAngio fusion protein in the targeted CWR22rv prostate cancer cell line and further augmented the biological activity of EndoAngio fusion protein to inhibit the proliferation, tubular network formation, and cell migration of human endothelial cells *in vitro*. These results suggest that this combination therapy significantly enhances the antiangiogenic effects of AdEndoAngio.

In animal studies, we observed a stronger therapeutic effect for the androgen-independent CWR22rv s.c. tumor model. AdEndoAngio and AdE4PESEE1a combination therapy was able to eliminate seven out of eight treated tumors. We believe that the potent antitumor effect resulted from a collaborative effort between AdEndoAngio and AdE4PESEE1a. Our previous study observed inefficient viral replication in AdE4PSESE1a-treated tumors that resulted in a tumor growth rate somewhat in advance of the tumor cell death rate, ultimately resulting in a failed therapy (3). In this study, AdEndoAngio coamplified with AdE4PSESE1a expressed a large amount of antiangiogenic factor, EndoAngio, to stop the growth of tumor cells, thus allowing AdE4PSESE1a enough time to eliminate the whole tumor mass by direct cell killing. Histologic results suggest that the residual tumor cells were in a necrotic condition. Cells showed increased eosinophilia, which was partly due to the loss of normal basophilia imparted by the RNA in the cytoplasm, and was partly due to the increased binding of eosin to denatured intracytoplasmic proteins (18). This result suggests that viral replication and the antiangiogenic factor together generated an environment highly unfavorable for tumor growth even when the therapy did not eliminate the tumor mass initially. A similar strategy was recently reported to treat androgen-independent C4-2 tumors (25). Jin et al. administered a tumor/tissue-restricted replicative adenovirus, Ad-hOC-E1, via tail vein injection and an antiangiogenic virus, Ad-Flk1-Fc, via intratumor injection. The combination modality using different viral administration methods probably did not give Ad-Flk1-Fc an adequate chance to amplify for better therapeutic effects.

Although coinjection of AdE4PSESE1a and AdEndoAngio can be used to treat locally advanced or recurrent prostate cancer, it is difficult to use this modality to treat metastatic prostate cancer. We are currently integrating the EndoAngio expression cassette into AdE4PSESE1a to make an antiangiogenic prostate-restricted replicative adenovirus for treating metastatic prostate cancer. Zhang et al. (20) recently reported the creation of an antiangiogenic oncolytic virus, ZD55-sflt-1, by inserting a soluble human vascular endothelial growth factor receptor, sflt-1(1-3), into an *E1B*-55-deleted oncolytic adenovirus vector. In that report, four of eight tumors were completely eradicated by incorporating ZD55-sflt-1 therapy with 5-fluorouracil therapy. However, that is only a 50% success rate. One possible reason for the lower therapeutic effect in that study compared with ours might be the relative potency of the antiangiogenic factors used. EndoAngio might have stronger antiangiogenic effects than sflt-1. Another possibility is that *E1B*-55-deleted adenovirus has a lower tumor-killing efficacy than AdE4PSESE1a. The *E1B*-55-deleted adenovirus, also known as mutant dl1520 or ONYX-015, is reported to selectively replicate in and kill cancer cells with mutations in the p53 gene or dysfunctional p53 gene product (26), but ONYX-015 has an attenuated oncolytic capacity compared with wild-type adenovirus as a consequence of *E1B*-55 kDa deletion (4). In addition, a recent report showed that the replication of

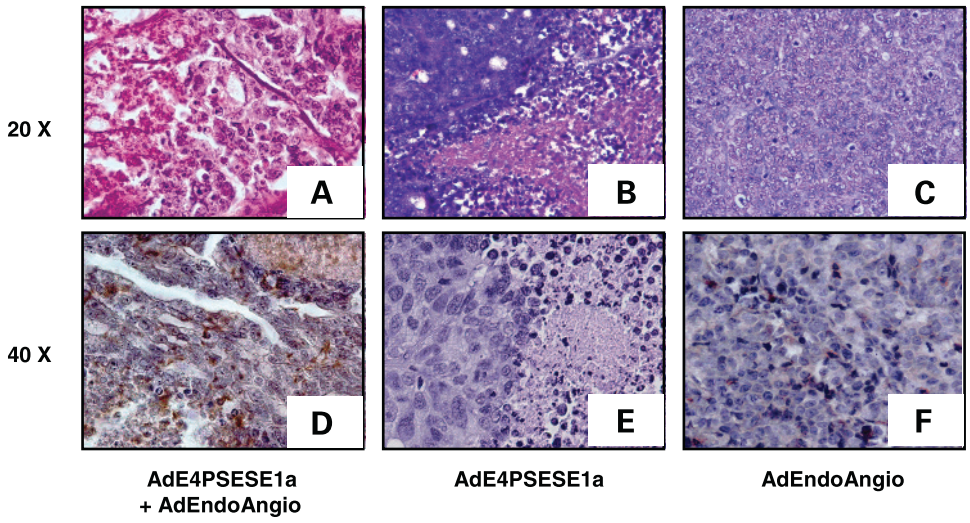

Figure 4. Histopathology of virus-treated tumors. Tumor masses were collected, formalin fixed, and paraffin embedded. Sections were subjected to H&E or immunohistochemical staining by anti-endostatin antibody. The tumor cells in the only residual tumor treated by combination therapy (**A**) was apparently undergoing necrosis, but the tumor cells in the remaining tumor were in an active growing condition in AdE4PSESE1a-treated tumors (**B**). The tumor cells showed normal morphology and no necrosis in the AdEndoAngio-treated tumors (**C**). Rich EndoAngio protein expression can be detected at the periphery of the tumor mass in the combination therapy group by immunohistochemistry (**D**), whereas no EndoAngio protein expressing cells were seen in the AdE4PSESE1a-treated tumors (**E**) and only limited positive-staining cells were observed in AdEndoAngio-treated tumors (**F**).

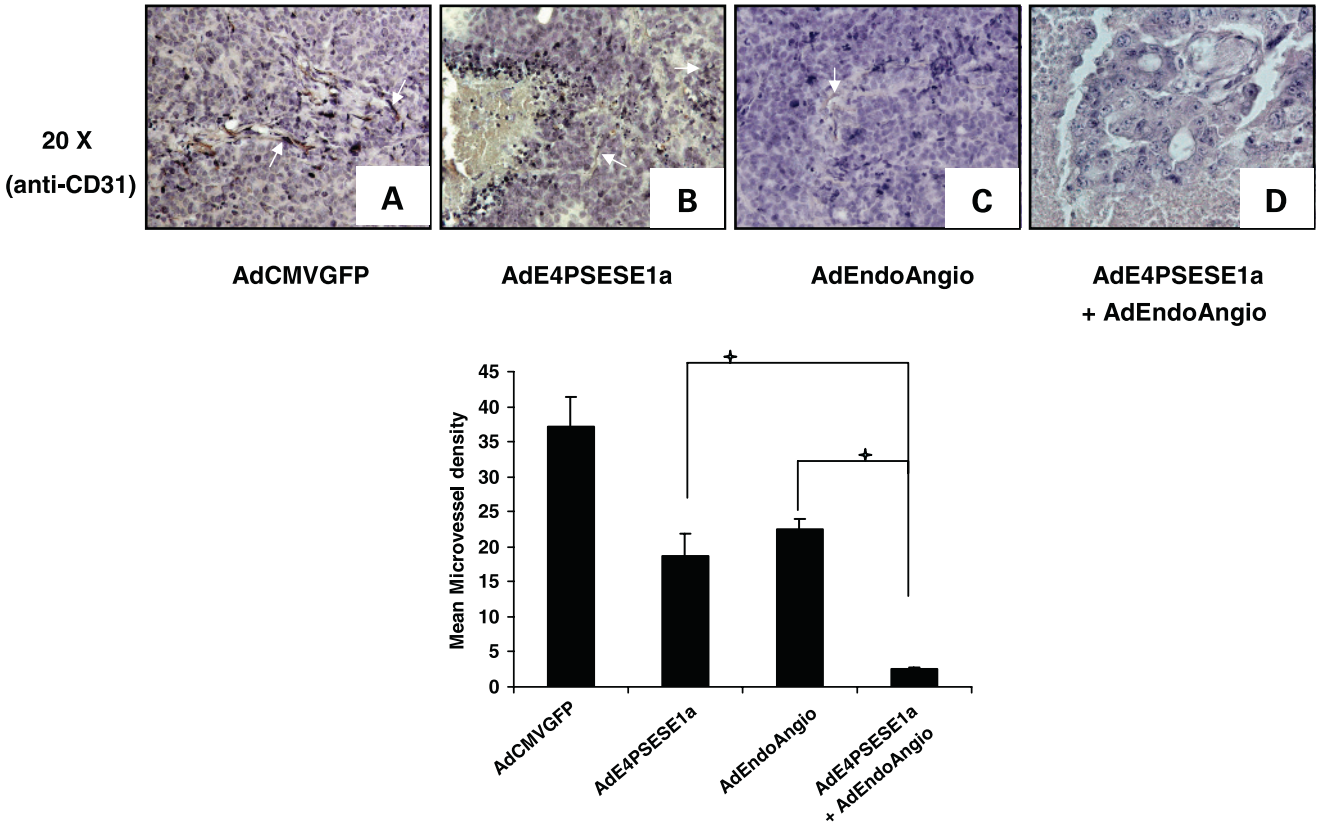

Figure 5. Quantification of capillaries inside the virus-treated tumors. The tissue sections above were used for immunohistochemical staining with anti-CD31 antibody to detect the capillaries. Quantification of CD31 antibody-labeled capillaries revealed a significant decrease in the residual tumor with combination therapy, compared with AdCMVGFP- or AdEndoAngio-treated tumors ($^{+}$, $P < 0.0001$). The results suggested that a stronger *in vivo* antiangiogenic effect is obtained when AdEndoAngio is coadministered with a prostate-restricted replicative adenovirus.

ONYX-015 does not depend on the p53 status of the target cell; instead, the capability of tumor cells to export viral late mRNAs is the main determinant of viral replication of ONYX-015 (27). It was also reported that not all tumor cells support the replication of ONYX-015 (28).

Although we observed significant therapeutic efficacy with the combination of oncolytic adenovirus plus replication-deficient adenovirus for advanced prostate cancer s.c. models in immunocompromised mice, the high prevalence of preexisting immunity to adenovirus 5 in patients may substantially limit its future clinical utility, despite the effect of both advanced prostate cancer and chemotherapy on immunocompetence. However, it should be possible to temporarily suppress the patients' immune system if the therapy is really effective in eliminating cancers. Alternatively, we can incorporate immune modulators such as Fas ligand into the gene therapy vectors to locally suppress the immune system.

In conclusion, we have developed a combination therapeutic modality for androgen-independent prostate cancer that was able to eliminate seven out of eight treated tumors by combining an antiangiogenic therapy and a prostate-restricted replicative adenovirus. The *in vivo* therapeutic efficacy suggests that using the autoangiogenic prostate-restricted replicative adenovirus is a promising strategy to treat androgen-independent prostate cancer and deserves more extensive investigation. Further developmental work is warranted for an antiangiogenic prostate-restricted replicative adenovirus strategy for treating metastatic prostate cancer.

References

1. Lee CT, Park KH, Yanagisawa K, et al. Combination therapy with conditionally replicating adenovirus and replication defective adenovirus. Cancer Res 2004;64:6660 – 5.

2. Matsubara S, Wada Y, Gardner TA, et al. A conditional replication-competent adenoviral vector, Ad-OC-E1a, to cotarget prostate cancer and bone stroma in an experimental model of androgen-independent prostate cancer bone metastasis. Cancer Res 2001;61:6012 – 9.

3. Li X, Zhang YP, Kim HS, et al. Gene therapy for prostate cancer by controlling adenovirus E1a and E4 gene expression with PSES enhancer. Cancer Res 2005;65:1941 – 51.

4. Oosterhoff D, van Beusechem VW. Conditionally replicating adenoviruses as anticancer agents and ways to improve their efficacy. J Exp Ther Oncol 2004;4:37 – 57.

5. Reid T, Warren R, Kirn D. Intravascular adenoviral agents in cancer patients: lessons from clinical trials. Cancer Gene Ther 2002;9:979 – 86.

6. Kirn D. Oncolytic virotherapy for cancer with the adenovirus dl1520 (Onyx-015): results of phase I and II trials. Expert Opin Biol Ther 2001;1:525 – 38.

7. Folkman J. Antiangiogenic gene therapy. Proc Natl Acad Sci U S A 1998;95:9064 – 6.

8. O'Reilly MS, Boehm T, Shing Y, et al. Endostatin: an endogenous inhibitor of angiogenesis and tumor growth. Cell 1997;88:277 – 85.

9. Blezinger P, Wang J, Gondo M, et al. Systemic inhibition of tumor growth and tumor metastases by intramuscular administration of the endostatin gene. Nat Biotechnol 1999;17:343 – 8.

10. Griscelli F, Li H, Bennaceur-Griscelli A, et al. Angiostatin gene transfer: inhibition of tumor growth *in vivo* by blockage of endothelial cell proliferation associated with a mitosis arrest. Proc Natl Acad Sci U S A 1998;95:6367 – 72.

11. Griscelli F, Li H, Cheong C, et al. Combined effects of radiotherapy and angiostatin gene therapy in glioma tumor model. Proc Natl Acad Sci U S A 2000;97:6698 – 703.

12. Sun X, Qiao H, Jiang H, et al. Intramuscular delivery of antiangiogenic genes suppresses secondary metastases after removal of primary tumors. Cancer Gene Ther 2005;12:35 – 45.

13. Habib NA, Mitry R, Seth P, et al. Adenovirus replication-competent vectors (KD1, KD3) complement the cytotoxicity and transgene expression from replication-defective vectors (Ad-GFP, Ad-Luc). Cancer Gene Ther 2002;9:651 – 4.

14. He TC, Zhou S, da Costa LT, Yu J, Kinzler KW, Vogelstein B. A simplified system for generating recombinant adenoviruses. Proc Natl Acad Sci U S A 1998;95:2509 – 14.

15. Schmitz V, Wang L, Barajas M, Peng D, Prieto J, Qian C. A novel strategy for the generation of angiostatic kringle regions from a precursor derived from plasminogen. Gene Ther 2002;9:1600 – 6.

16. Schleef RR, Birdwell CR. The effect of fibrin on endothelial cell migration *in vitro*. Tissue Cell 1982;14:629 – 36.

17. Gleave M, Hsieh JT, Gao CA, von Eschenbach AC, Chung LW. Acceleration of human prostate cancer growth *in vivo* by factors produced by prostate and bone fibroblasts. Cancer Res 1991;51:3753 – 61.

18. Cotran RS, Kumar V, Collins T. Robbins pathologic basis of disease. 6th ed. Philadelphia: W.B. Saunders; 1999. p. 16.

19. Zhang Q, Nie M, Sham J, et al. Effective gene-viral therapy for telomerase-positive cancers by selective replicative-competent adenovirus combining with endostatin gene. Cancer Res 2004;64:5390 – 7.

20. Zhang Z, Zou W, Wang J, et al. Suppression of tumor growth by oncolytic adenovirus-mediated delivery of an antiangiogenic gene, soluble Flt-1. Mol Ther 2005;11:553 – 62.

21. Liu XY, Qiu SB, Zou WG, et al. Effective gene-virotherapy for complete eradication of tumor mediated by the combination of hTRAIL (TNFSF10) and plasminogen k5. Mol Ther 2005;11:531 – 41.

22. Selleck WA, Canfield SE, Hassen WA, et al. IFN-γ sensitization of prostate cancer cells to Fas-mediated death: a gene therapy approach. Mol Ther 2003;7:185 – 92.

23. Sauter BV, Martinet O, Zhang WJ, Mandeli J, Woo SL. Adenovirus-mediated gene transfer of endostatin *in vivo* results in high level of transgene expression and inhibition of tumor growth and metastases. Proc Natl Acad Sci U S A 2000;97:4802 – 7.

24. Calvo A, Feldman AL, Libutti SK, Green JE. Adenovirus-mediated endostatin delivery results in inhibition of mammary gland tumor growth in C3(1)/SV40 T-antigen transgenic mice. Cancer Res 2002;62:3934 – 8.

25. Jin F, Xie Z, Kuo CJ, Chung LW, Hsieh CL. Cotargeting tumor and tumor endothelium effectively inhibits the growth of human prostate cancer in adenovirus-mediated antiangiogenesis and oncolysis combination therapy. Cancer Gene Ther 2005;12:257 – 67.

26. Bischoff JR, Kirn DH, Williams A, et al. An adenovirus mutant that replicates selectively in p53-deficient human tumor cells. Science 1996;274:373 – 6.

27. O'Shea CC, Soria C, Bagus B, McCormick F. Heat shock phenocopies E1 – 55K late functions and selectively sensitizes refractory tumor cells to ONYX-015 oncolytic viral therapy. Cancer Cell 2005;8:61 – 74.

28. Shen Y, Kitzes G, Nye JA, Fattaey A, Hermiston T. Analyses of single-amino acid substitution mutants of adenovirus type 5 E1 – 55K protein. J Virol 2001;75:4297 – 307.